Chapter 16: Cranktrain (Crankshafts, Connecting Rods, and Flywheel)

16.1 Definition of Cranktrain Function and Terminology

The Cranktrain is the heart of the reciprocating piston engine, and the purpose is to translate the linear motion of the pistons into rotary motion for the purpose of extracting useful work. This is typically composed of a connecting rod, crankshaft, and flywheel or power takeoff device. The actual realization of these parts take on many forms, and the description and physics of these were covered in Chapter 6.

The crankshaft is usually composed of one or multiple throws, to which the connecting rod is attached with either fluid film journal bearings or rolling element bearings as shown in **Figure 16.1**. The crankshaft is typically cast or forged of iron or steel. In addition to its main function of translating linear to rotary motion, the crankshaft typically drives many of the engine accessories such as: valvetrain, lube system, cooling system, or charging system. Crankshaft rotation direction can be either clockwise or counterclockwise, depending on driveline packaging and requirements. It can rotate in both directions in some applications, if the valvetrain mechanism is designed appropriately. One example would be golf carts, where the two stroke engine drives the vehicle forward, and can be stopped and restarted in the opposite direction to provide a means of reverse. The crankshaft typically incorporates additional balance weights to smooth the vibration produced by the oscillating of the piston.

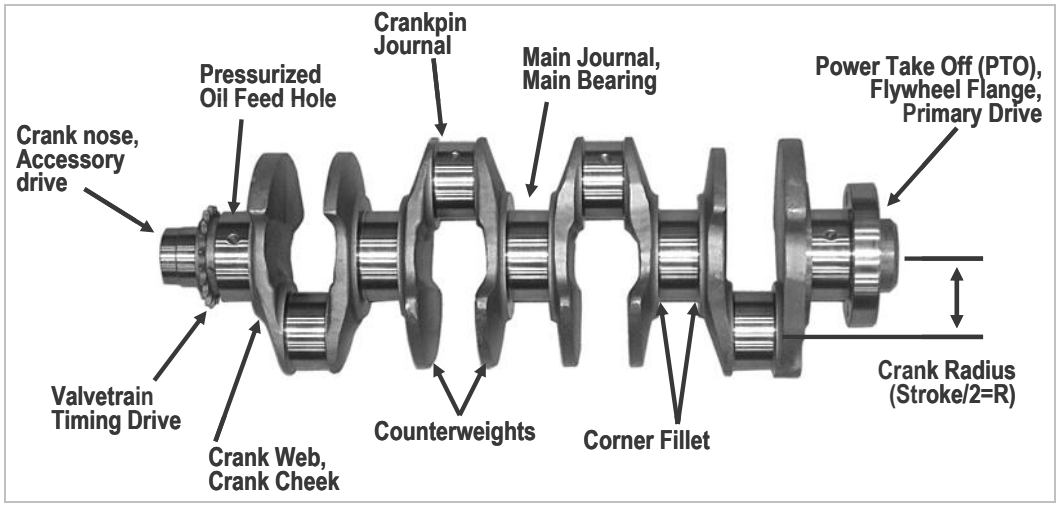

Figure 16.1: Crankshaft Terminology

The connecting rod in its simplest form is a beam with two pin joints at either end, as shown in **Figure 16.2**. One end sees relatively low rotation speeds as it is connected to the piston, while the other sees high rotation speeds as it is attached to the crankshaft. The connecting rod will typically support the bearings or bushings for both ends of its application. It is one of the most stressed components in the engine and subjected to high tensile, compressive, and bending stress. It can be cast, forged, or sintered from powdered metal.

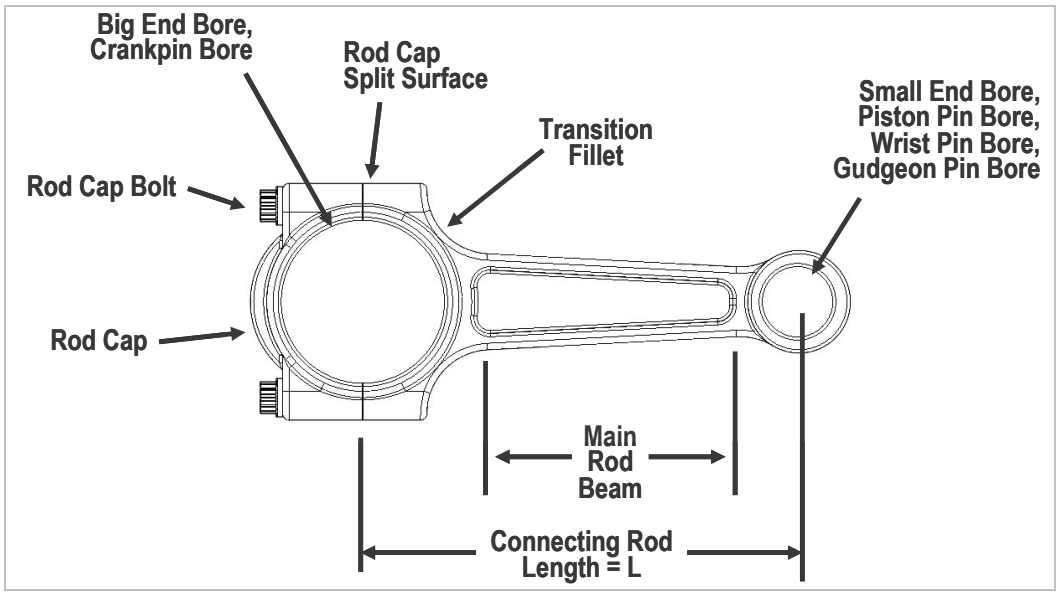

Figure 16.2: Connecting Rod Terminology

The flywheel provides a variety of functions. As the name implies, it adds additional rotating inertia to the crankshaft, to smooth out the cyclical speed variation produced by the reciprocating piston schedule. This is most important at idle for minimizing torsion vibration to the engine, and for ease of fuel calibration. When attempting to move a vehicle from stationary, the flywheel provides energy to overcome the inertia of the vehicle for smooth starts. If the inertia of the cranktrain is too low, the engine may stall or unnecessarily high RPM will be required to launch the vehicle from rest. A further function of the flywheel is often the power takeoff, as it provides a friction surface for the clutch to act against, or the torque converter to mount to, as shown in **Figure 16.3**.

Figure 16.3: Flywheel mounted to crankshaft

As the cranktrain geometry is part of the initial engine layout, and composes a significant portion of the engine cost, it is important to plan ahead for future product improvements. Often this includes increases in engine bore or stroke to increase

displacement, addition of supercharging, and/or an increase in engine speed. The additional cost of package protecting for product improvements must be balanced against the potential increases in cost or weight of a given component, and against the cost of an engine redesign at a later date. One possible strategy could be to release the initial engine design with cast components, and later upgrade to forged ones.

16.2 Operating Environment Considerations

Typical ambient temperatures are from -30ºC to 50ºC. It is important when sizing bearing fits, or considering material properties, to plan for the temperatures that the engine will see at startup. It may also be important to consider bearing fits at temperatures well below operating temperatures, to prevent component yielding while in storage.

Operating temperatures of the crankshaft and connecting rod are typically oil operating temperature of between 80-110ºC, but peak oil temperatures can rise to 150ºC. Connecting rod crankpin bore temps are similar, but piston pin end temperatures are higher as they are exposed to the bottom side of the piston. The connecting rod piston pin end typically sees 150-180ºC. Flywheel temperatures will depend on location in the engine, and exposure to cooling airflow. They can vary from: the same temperature as the crankshaft, lower with cooling air flow, to higher with frequent clutch engagement.

The crankshaft and connecting rods are typically immersed in an oil bath in the cylinder block. As a by product of combustion, water and sulfuric acid are present and often work past the piston rings into the oil bath.

In addition to the safety factor calculations made with respect to fatigue life of material, duty cycle must be considered. Some engines such as over-the-highway truck, locomotive, ship, generators, lawn equipment, and racing engines may operate close to maximum load for most of their operating lives. While passenger car engines may spend less than 0.1% of their useful life at maximum load. The cranktrain is typically one of the more expensive assemblies in an engine, and when it breaks it frequently damages other components in the engine (cylinder block, cylinder heads, piston, valvetrain). Therefore high reliability is needed from the crankshaft design.

16.3 Description of Common Cranktrain Configurations and Architectures

16.3.1 Crankshaft Configurations

Crankshafts typically fall into single or multiple throw configurations, with single or shared journals for connecting rods. A single throw crankshaft is typically used in single or twin cylinder applications, with either a single rod per journal or two. A multiple throw crankshaft can be used for a two cylinder engine, but is typically used for

three or more cylinders. Inline engine configurations use a single rod per throw, while vee engines usually have two rods per throw.

Multi-throw crankshafts are typically arranged in a single plane or multiple planes. A single-plane or flat-plane crankshaft is where all crankpin throws are at either 0º or 180º, as on in inline four cylinder engine as shown in **Figure 16.4**. A multi-plane arrangement is where the crankpin throws are arranged in different planes. A two-plane crankshaft (cross, cruciform) is where the throws are indexed 90º apart as on the V-8 engine shown in **Figure 16.5**, or three-plane like on a six cylinder engine.

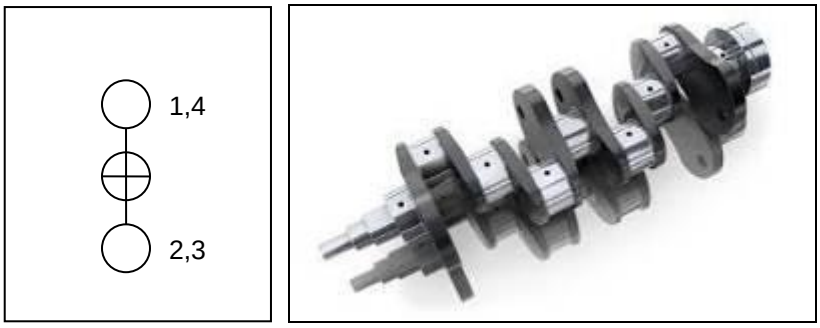

Figure 16.4: Single-plane crankshaft

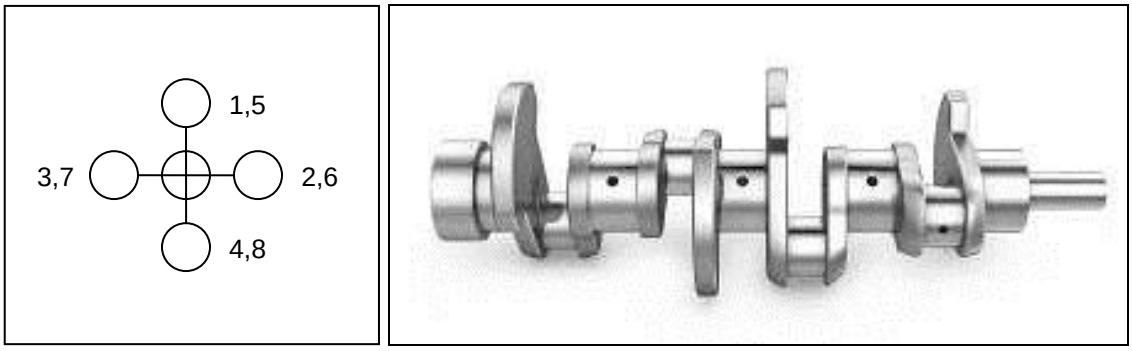

Figure 16.5: Dual-plane crankshaft

In addition to the forces and loads, there are various other design considerations:

- One piece or assembled crankshaft
- Bearing type (rolling element or journal bearing)
- Integral or separately attached counterweights (racing)
- Type of power take-off
- Accessory drive location and type
- Cost versus weight
- Duty cycle
- Volume and manufacturing methods

16.3.1.1 Assembled or Built-up Crankshafts

An assembled crankshaft is one composed of multiple pieces that were manufactured separately, then joined together to form a single crankshaft by means of a

press fit, bolted, or welded joint. A single cylinder, 2-stroke crankshaft is shown in **Figures 16.6**.

Figure 16.6: Assembled crankshaft

An assembled crankshaft is typically used on either very small or very large engines to ease the manufacture. The manufacture of small crankshafts, typically single throw, can be made less expensive since the creation of multiple circular pieces are made on a simple lathe and are then centerless ground. This does not require a more expensive offset crankshaft grinding machine. Additionally, this makes manufacture of very large crankshafts for ships and stationary pumping engines easier, as they can be made of more easily managed 'small' pieces.

Another key advantage of the assembled crankshaft is the ability to employ rolling element bearings, which reduce engine friction and ease lubrication requirements. The elements of the crankshaft can be assembled around a rolling element bearing and connecting rod assembly. This is common in 2-stroke engines, where splash lube or vapor lube are used to enable rolling element bearings and eliminate the need for pressure lubrication. The assembled crankshaft also allows the cylinder block to be vertical or horizontal split into two halves.

One of the key challenges for the assembled crankshaft is aligning all of the sub-components during assembly to a high tolerance. This usually requires the application of large force to assemble and then straighten the components to achieve the desired straightness of the crankshaft for the alignment of bearings. The key failure mode of an assemble crankshaft is the misalignment of these components during operation. The torque of the engine may cause the assembled joints to slip with respect to one another, and "scissor", leading to misalignment of the crankshaft.

16.3.1.2 One Piece Crankshaft

A one piece crankshaft is typically cast or forged as a single unit, then machined and ground to achieve the final geometry as shown in **Figure 16.7**. This method of manufacture is advantageous for larger volume production which justifies the investment

in casting or forging tooling, and dedicated offset crankshaft grinding equipment. One piece crankshafts are not typically straightened, which is an advantage over an assembled crankshaft in a multiple cylinder engine. Some V-8 crankshafts are cast as flat plane, and then twisted to cross plane while still hot.

The disadvantage of this type of crankshaft is that only plain bearings can be used, and pressure fed lubrication and cross drillings are required. This typically forces the cylinder block to be split along the bearing centerline, and affects overall engine architecture.

Figure 16.7: One piece crankshaft

16.3.2 Connecting Rod Configurations

There are four basic configurations for the crankpin bore of the connecting rod as shown in **Figures 16.8-16.11**. These vary in geometry according to function.

1. Plain (most common),
2. Angled split (for serviceability),
3. One piece (for rolling element bearings), and
4. Articulated (for radial engines).

Figure 16.8: Plain connecting rod

Figure 16.9: Angled split connecting rod

Figure 16.10: One piece connecting rod

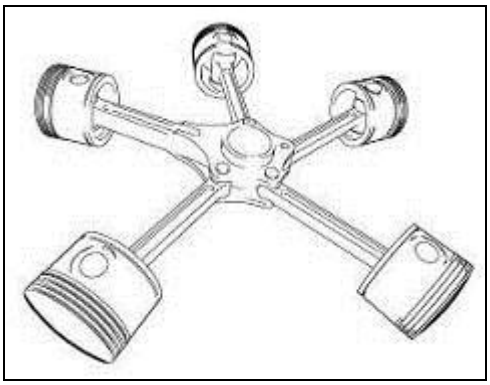

Figure 16.11: Articulated connecting rod

The plain connecting rod is most common in current automotive practice. It allows addition of bearings of a different material type than the connecting rod. An angle split connecting rod allows it to be removed through the top of the engine, which helps rebuild of engines while the cylinder block is still in the vehicle. This is common in over the highway trucks and locomotives, which have a large crankpin and consequently large bearing. A disadvantage of an angled split rod is non symmetrical loading of the connecting rod crankpin bore. The rod cap is now at an angle to the loading, and it makes the cap slide with respect to the upper rod, thus requiring additional attention to cap locating.

A one piece connecting rod enables a rolling element bearing to be used to reduce engine friction. However, the application of a one piece connecting rod is usually limited to engines with an assembled crankshaft, to provide access to assemble the bearing and crankpin through the middle of the connecting rod. A one piece connecting rod is lighter and less expensive than a plain rod since rod cap fasteners are not required, however a bearing quality surface is required on the crankpin end, since the rollers ride directly on the rod.

An articulated rod is used for radial engines where more than one connecting rod must attach to the same crank journal. This arrangement reduces the axial length of the crankpin journal for multiple cylinders, and is most common in air-cooled radial aircraft engines. All connecting rods attach to the same crankpin to allow all cylinders to face the cooling airflow equally.

Regardless of crankpin bore arrangement, the job of the connecting rod is to keep the crankpin bearing as round as possible to ensure an even oil film and prevent contact of the rod bearing to the crankshaft. The connecting rod cap may have reinforcing ribs to increase stiffness, as shown in **Figure 16.12**. A single rib is easiest to cast or forge, but a double rib is a more efficient distribution of stiffness.

Figure 16.12: Rib on connecting rod cap

There are two general configurations of connecting rod beam cross-section as shown in **Figure 16.13-16.14**. The beam is the portion of the connecting rod that connects the piston pin and crankpin ends, and when viewed in cross section resembles a capital letter "I" or capital letter "H".

Figure 16.13: I-beam

Figure 16.14: H-beam

The I-Beam connecting rod is most common in use because it puts the most material in the areas of maximum bending stress while reducing material where it is not needed. The I-Beam shape also lends itself well to the casting, forging, or Powdered Metal (PM) processes. The pull direction for the beam is in the same direction of the pin bosses, making forming easier and reducing the requirement for material removal.

The H-Beam connecting rod is more difficult to manufacture, but this geometry offers a more stable, lighter design. The H-beam rod allows a more gradual transition of stiffness between the main beam and the crankpin end of the connecting rod, reducing stress in this critical radius. It also has greater bending stiffness in the crankpin axial direction than an I-bean rod. This may lead to increased edge loading on the crankpin bearing, when two rods share the same journal. Due to the added expense of manufacture, this is usually only seen in competition engines.

A hollow beam connecting rod could result in the lowest possible connecting rod weight for a given stiffness. While the hollow beam does not offer any benefit in tension, it better resists column buckling in compression and bending stress caused by rod whip. However, manufacturing of this rod is difficult and limits its application in practice. This geometry could be generated from a weldment of several pieces, or a core could be used in a cast rod.

The small boss that interfaces with the piston pin typically utilizes a pressed bushing. If a bushing is not used, a coating is required on one of the two mating components to reduce wear. This end of the rod sees relatively low rotation speed, and reverses direction between TDC and BDC, resulting in solid friction or mixed lubrication. Geometry of the piston pin end varies between straight sides and tapered, depending on anticipated engine operating speed and inertial loads, as shown in **Figure 16.15**. Occasionally an oil feed hole is added for the connecting rod piston pin bushing to improve lubrication; either as a passive splash oiling hole or pressure lube up from the crankpin bearing.

Figure 16.15: Pressed small end bushing, tapered piston pin end geometry, splash oil hole

16.3.3 Flywheel Configurations

The most common arrangement of flywheel in automotive is a separate disc attached to the end of the crankshaft, usually by a bolted joint. The total cranktrain inertia is composed of flywheel, crankshaft, rotating mass of connecting rods, crank pulley for driving accessories, and clutch or torque converter. Occasionally the flywheel is incorporated as part of the crankshaft counterweights, the disc varying in thickness to achieve the desired balance counterweight. This is common practice in motorcycle applications as shown in **Figure 16.16,** and 2-stroke engines. The flywheel may also serve additional functions such as a power take off (clutch or torque converter interface), as a drive mechanism for the starter, or as a tone wheel for electronic engine controls.

Figure 16.16: Flywheel integrated with crankshaft counterweight

16.4 Detailed Design of Crankshaft Geometry

During the concurrent engine design process, the design of the cranktrain is not a linear process from point A to point B. As the design of the overall engine evolves, so must the cranktrain design. However, there is a general flow to the steps taken to calculate loads and design a crankshaft for a single throw crankpin as shown in **Figure 16.17**. While actual stress can be calculated by classical methods, most will use Finite Element Analysis once loads are known.

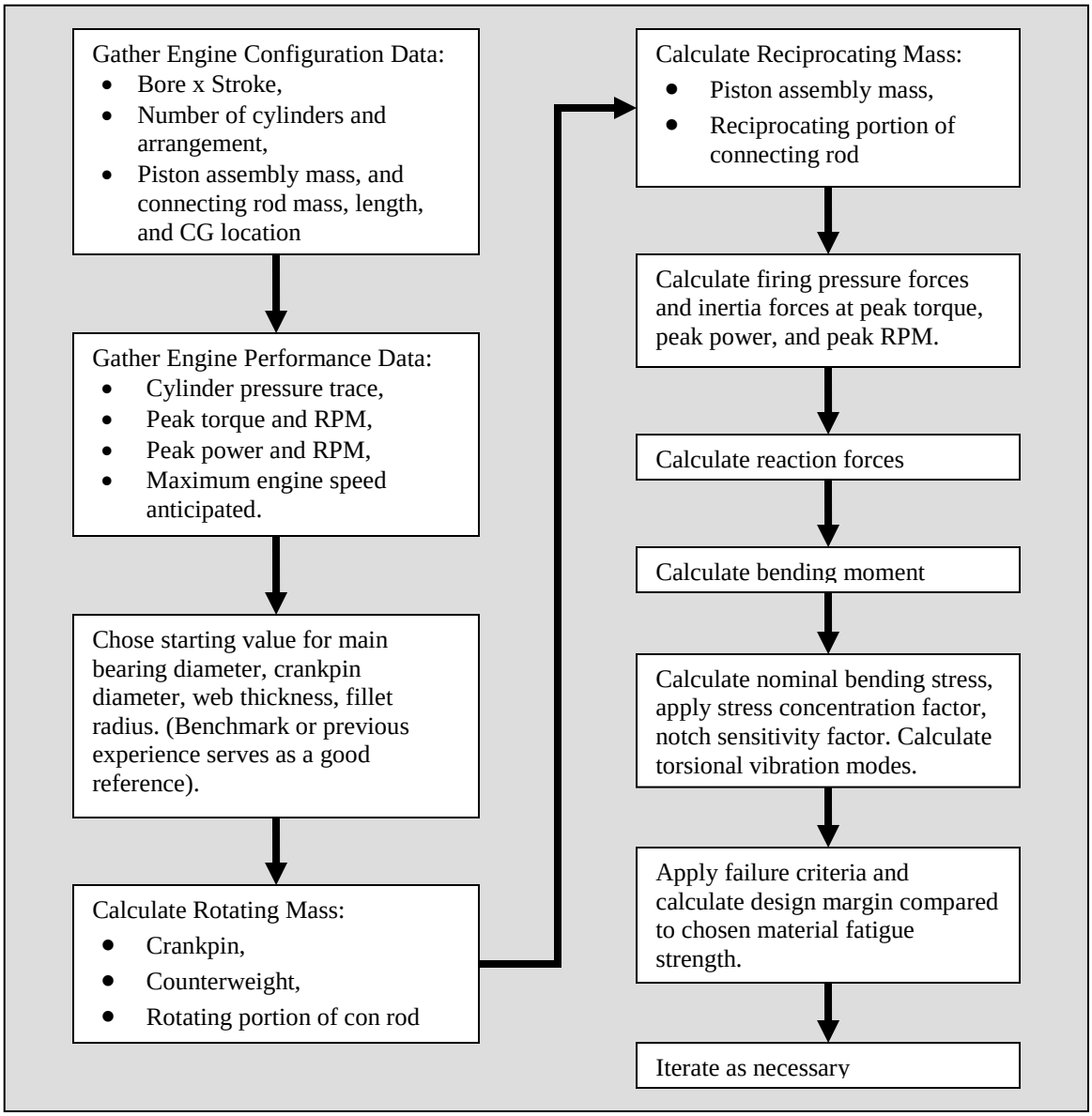

Figure 16.17: General steps to designing a crankshaft

16.4.1 Detailed Design of Crankshaft Geometry

The geometry of a crankshaft is complicated, and the loading varies as a function of its rotational position. Because of the dissimilar cross-sections of the crankshaft, it will be sensitive to discontinuities in stiffness. It is at these stiffness discontinuities that stress will be concentrated. Generally, the crankshaft fillet will be the most highly stressed area and will require the most detailed design attention as the materials used to make crankshafts are typically sensitive to notch factors. Loading at the fillet alternates as shown in **Figure 16.18-16.19**; TDC-Firing puts the crankpin in compression, and TDC-Overlap puts the crankpin in tension. Stress in this area is further magnified by torsional vibration, to be discussed later. Often metal improvement processes, such as shot peening

or fillet rolling, are used to introduce residual compressive stress at the fillet radii to improve fatigue life.

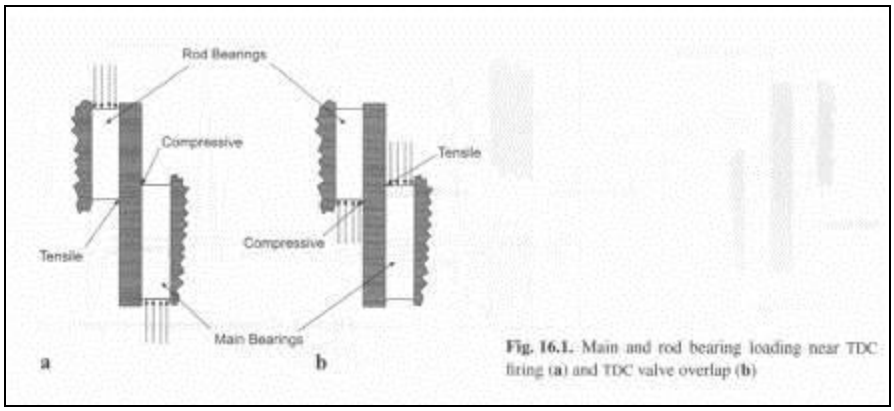

Fig. 16.1. Main and rod bearing loading near TDC firing (a) and TDC valve overlap (b)

Figure 16.18: Main and rod…

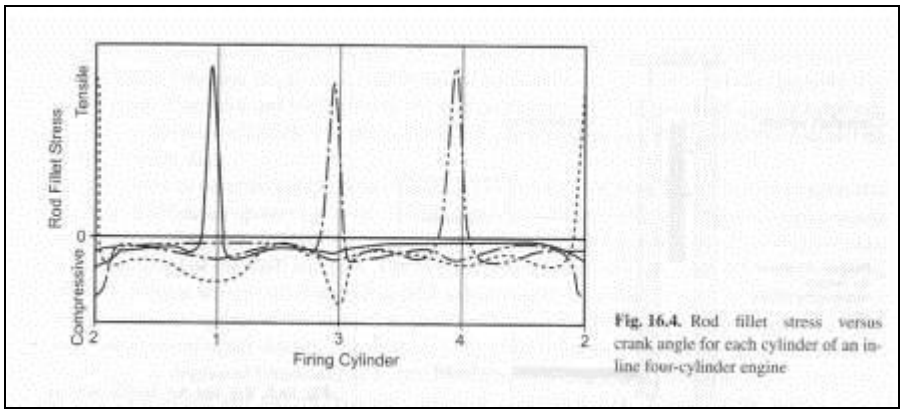

Fig. 16.4. Rod fillet stress versus crank angle for each cylinder of an in-line four-cylinder engine

Figure 16.19: Rod fillet stress….

Pin overlap, crank web thickness, and journal fillet radius are the key parameters that are varied in crankshaft design. As illustrated in **Figure 16.20**, a crankshaft that gets it's stiffness from pin overlap (large journal diameters and short stroke) does not need much crank web thickness, if at all. While a crankshaft that has little or no pin overlap will required a thicker crank web to gain stiffness. Depending on the geometry of the crank, it will be more sensitive to web thickness or pin overlap, as displayed in **Figure 16.21**. Cross drillings or hollow sections in the crankpin and main journals can reduce the pin stiffness and minimize the stiffness discontinuity that leads to a stress concentration.

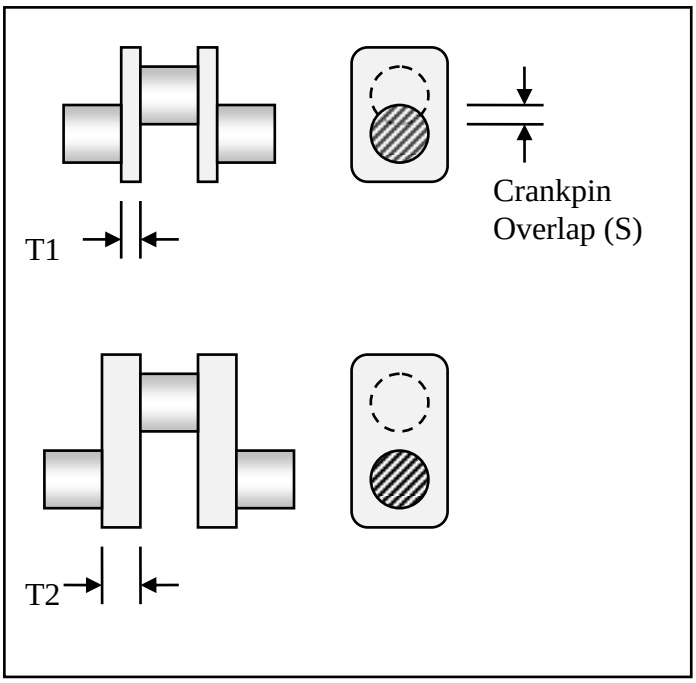

Figure 16.20: Pin Overlap vs. Web Thickness

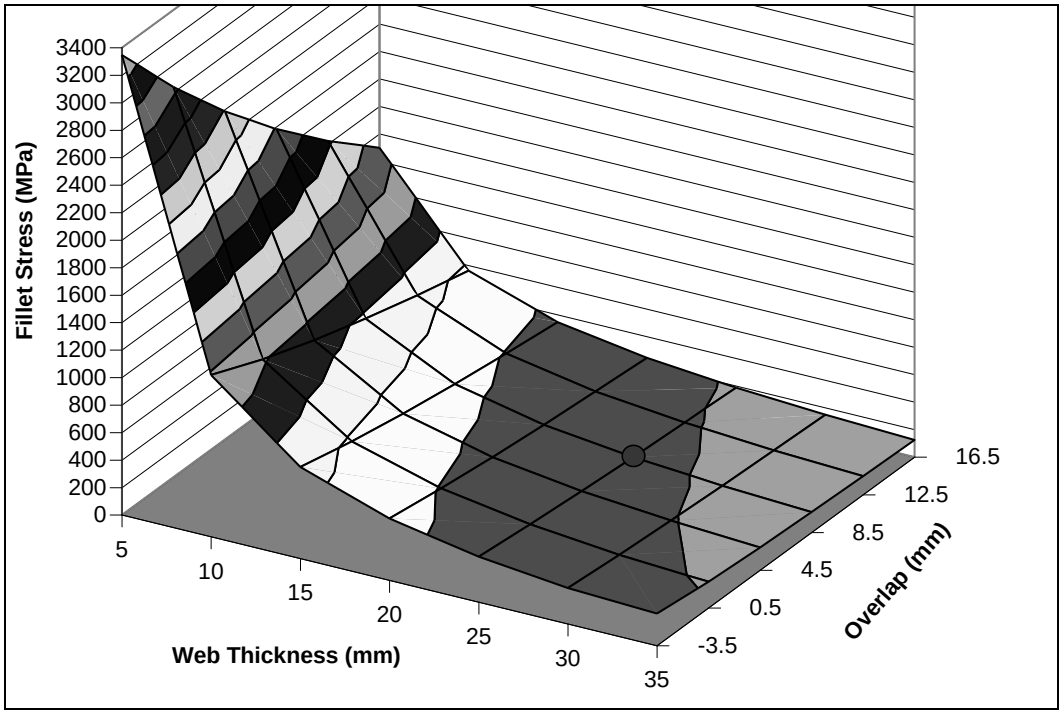

Figure 16.21: Effect of crankpin overlap (S), web thickness on crankpin fillet stress due to firing pressure

One way to increase pin overlap, is to increase journal bearing diameter for a given engine stroke, as shown in **Equation 16.1**. This will help crank stiffness, but increasing pin diameter increases fluid film friction at the bearings and reduces net engine power, and increases fuel consumption. It also increases crankshaft weight as the

increase mass of the crankpin will need to be offset by increasing mass in the counterweights.

$$S_{Overlap} = \frac{\left(D_{crankpin} + D_{Main} - Stroke\right)}{2} \qquad (16.1)$$

Where:

$S_{overlap}$ = Pin overlap
$D_{crankpin}$ = Diameter of the crankpin journal
D_{main} = Diameter of the main bearing journal

Fillet radii have enormous effects on the maximum stress in the crankshaft. Once the basic proportions of the crank have been determined, the choice of these radii is critical. The larger the fillet that can be used on the crankpin or main journal, the less the stress concentration notch factor will be. However, the larger the journal fillet, the less surface area is available for the connecting rod or main bearing as shown in **Figure 16.22**.

Several things can be done to minimize the stress at these fillet radii, but at additional cost. The geometry can be improved by using an undercut fillet as also shown in **Figure 16.23** to increase the effective radius. The material properties can be improved by introducing residual compressive stresses by fillet rolling or shot peening the fillet radius.

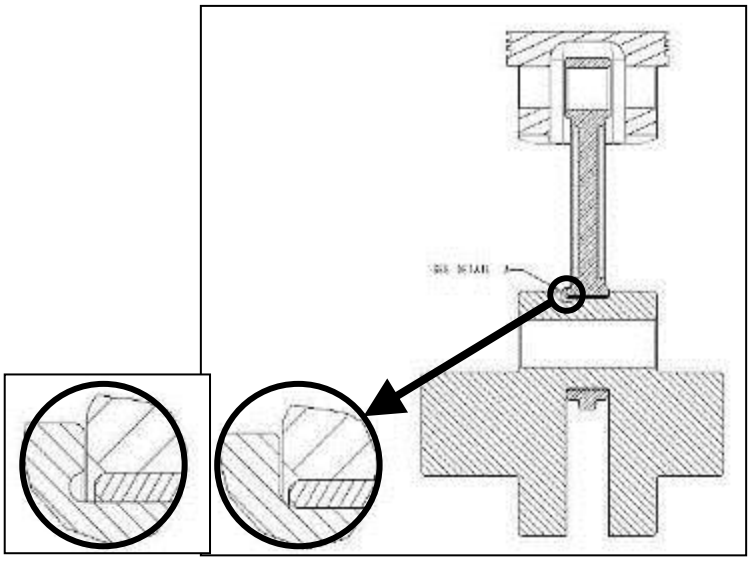

Figure 16.22: Crank fillet radius, Undercut fillet

Figure 16.23: Undercut fillet at crankshaft main bearing journal (middle)

16.4.2 Crankshaft Initial Sizing Values

When designing a new crankshaft, it is useful to have a starting point. This can come from benchmarking of successful crankshafts in similar applications, or from initial sizing values. These initial sizing values for the crankshaft were developed in the 1930's and 1940's in an era before computer aided design, and were developed by loading crankshafts and measuring displacement with extensometers or strain gauges. In modern practice, initial values will be assumed and the design will progress to FEA.

Initial sizing guidelines are listed in **Table 16.1** and illustrated in **Figure 16.24** below. These values are given as a function of cylinder bore diameter. When designing a crankshaft, it is important to make sure that the stroke and crankpin length don't interfere with the cylinder bore in the cylinder block, which might require raising the deck height of the cylinder block.

Table 16.1: Initial Sizing Values

Feature	Initial Sizing Value
Cylinder bore diameter	D
Cylinder spacing	1.20*D
Crankpin diameter	>0.6*D
Crankpin journal width	0.35*D, width/dia.>0.3
Main journal diameter	0.75*D, > pin dia.
Main journal width	0.40*D, width/dia.>0.3
Web (cheek) thickness	0.25*D
Crankpin fillet	0.04*D, >0.05*journal dia.
Main fillet	0.04*D

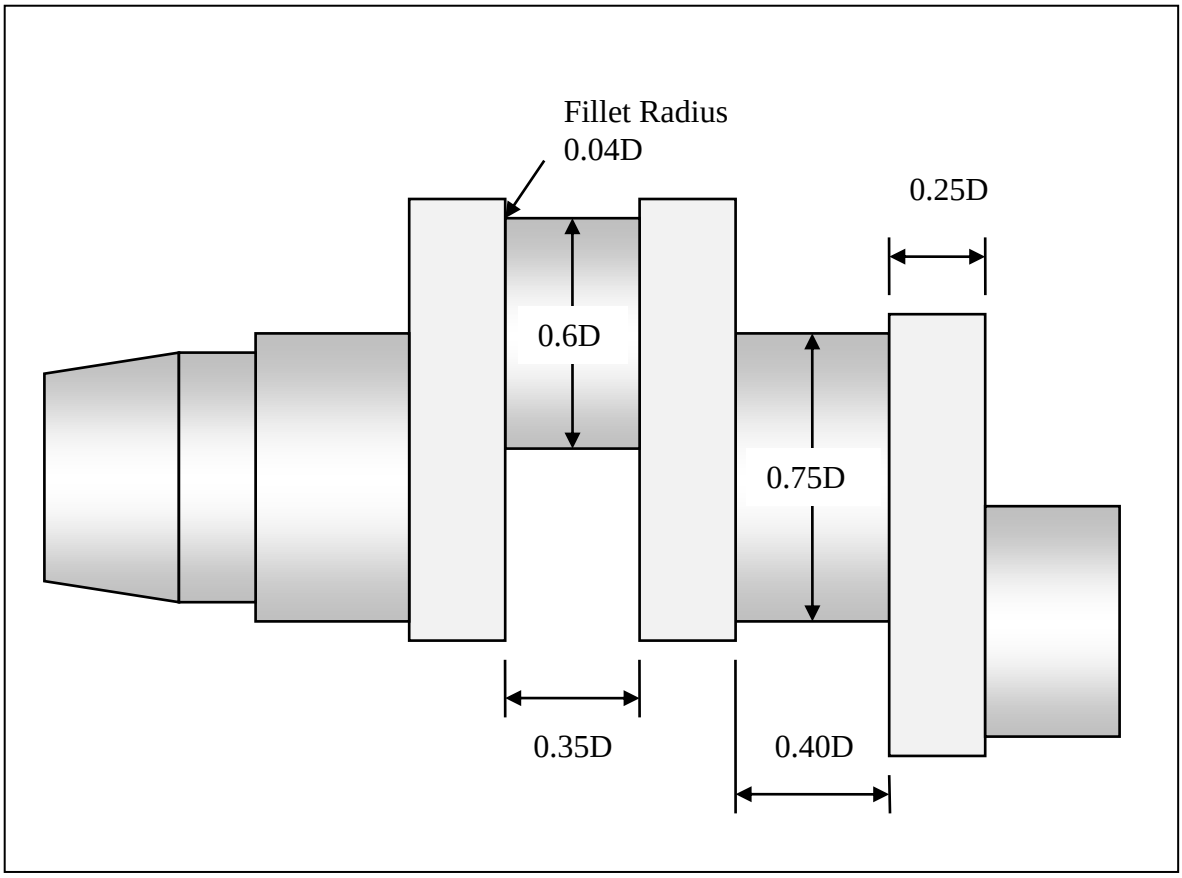

Figure 16.24: Initial sizing values

The majority of external loads are applied to the crankshaft perpendicular to its rotational centerline, and the reaction forces are thus transmitted through the rod and main bearings. However, in addition to these loads the crankshaft is exposed to some thrust loading – loading applied along the axis of crankshaft rotation. Thrust loads occur as the clutch in a manual transmission application is engaged or disengaged. With an automatic transmission, the load transfer through the torque converter includes a thrust component. If the camshaft is driven with a gear train using helical gears a further thrust load is transmitted to the crankshaft. As the engine fires, the crankshaft throw deflects, and the main bearings spread axially. Finally, dimensional stack-up between the crankshaft and the connecting rods and cylinder bore centerlines results in a small thrust load. For all of these reasons the crankshaft must include a thrust bearing surface. This is typically provided in conjunction with one of the main bearings. Because the largest thrust loads are generated at the rear of the crankshaft the thrust bearing is often placed at or near the rear main bearing; for packaging reasons the second-to-rear main bearing is often used since the rear main bearing must also incorporate the rear oil seal. If the crankshaft stiffness is sufficient the middle main bearing may be chosen. This is done because the machined thrust surface provides the fore and aft datum for crankshaft machining. Placing this datum in the middle of the crankshaft allows the fore and aft tolerances to be split equally between the front and rear portions of the crankshaft, making machining process control easier.

16.4.3 Crankshaft Natural Frequencies

Torsional vibration results whenever an unsteady or cyclical load is applied to a spinning shaft. A number of components in engines, including camshafts, water and oil pump drives, various accessory drives, and the crankshaft meet the criteria for potential torsional vibration problems. Of these the crankshaft receives by far the most attention since the combination of the length of the shaft and the magnitude of the forces result in the most severe conditions. Torsional vibration increases the stresses in the crankshaft webs, and the resulting oscillation of the crankshaft nose loads and unloads the camshaft and accessory drives. The latter significantly increases drive wear and engine noise. In heavy-duty engines camshaft torsional vibration is receiving increasing attention, and examples of vibration problems in accessory drives can be readily found. The focus in this section will be on the crankshaft, but many of the principles discussed here can be applied to other components.

In **Figure 16.25** the fundamental concepts of torsional vibration are summarized, as well as in **Equation 16.2**. Looking at this simple case a disk of some appreciable mass is rigidly mounted at the end of a shaft, the other end of which is mounted to prevent it from spinning. A torque is then applied to the disk to rotate it slightly from its initial position, elastically deforming (twisting) the shaft. The torque is then suddenly released, and the shaft unwinds. The shaft seeks to return to its original non-deformed state, but the mass of the disk results in an overshoot and the shaft is twisted in the opposite direction. The disk will oscillate back and forth at the natural frequency of the system, with decaying amplitude in each successive oscillation. The natural frequency is determined by the mass of the disk and the stiffness of the shaft.

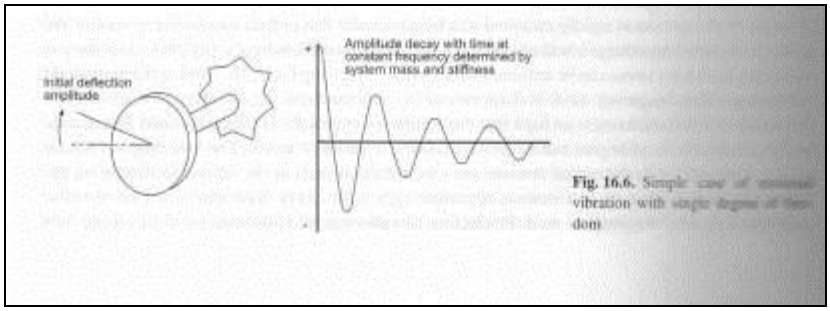

Figure 16.25: Simple case of…

$$k_r = \frac{G \cdot J}{L} = \frac{\pi d^4 G}{32 L} \qquad (16.2)$$

Where:

k_r = Torsional spring constant of the shaft
d = Diameter of shaft
G = Shear Modulus
L = Length of shaft

If the shaft consists of several sections of different diameters, as in a stepped shaft or crankshaft, the equivalent torsional spring constant can be calculated in same way as for springs in series as shown in **Equation 16.3**:

$$\frac{1}{k_{eq}} = \frac{1}{k_{r1}} + \frac{1}{k_{r2}} + \cdots \tag{16.3}$$

The natural frequency can be modeled using **Equation 16.4**:

$$\omega_n = \sqrt{\frac{k_{eq}}{I}} \tag{16.4}$$

Where:

I = Inertia of Disc

The case just described can now be extended in two important ways. First, one can imagine that the shaft and disk are spinning at some constant speed and that the torque is applied to and released from the spinning disk. In this case the resulting oscillation of the disk will be superimposed on the mean speed of the shaft and disk. The next extension is to consider a case where the spinning shaft has not one but several disks, and at various points in time sudden torque impulses are applied in succession to various of the disks. The problem has now become appreciably more complex as different portions of the shaft twist and untwist relative to other portions. Where the first two cases each had one ***degree of freedom*** and a single ***natural frequency*** this third case has an additional degree of freedom and natural frequency for each additional disk. Assuming the mass of each disk, and the shaft stiffness between each disk, are known, and assuming that the torque impulses applied to each disk can be characterized as a function of time the torsional vibration can still be calculated. The resulting matrix of equations is difficult to solve by hand, but can readily be addressed with computer calculations.

The third case just described is exactly that of the crankshaft in a multi-cylinder engine. In order to address crankshaft torsional vibration it is necessary to characterize both the crankshaft system and the system excitation – in this case the torque applied to the system at each cylinder.

Turning first to the crankshaft system it is helpful to characterize this system as a series of disks connected by stiff springs as shown in **Figure 16.26**. Each disk represents the rotating mass associated with a portion of the crankshaft system. The first disk represents the crankshaft nose, vibration dampener, and accessory drive pulleys. Disks two through seven represent the cylinders of this in-line six-cylinder engine. The eighth disk represents the flywheel or torque converter. It should be noted that the transmission and the remainder of the drivetrain are not represented. This is an accurate approach in automotive engines because transmission of torsional vibration is minimized through the fluid coupling in the torque converter and the clutch pack typically has a torsional compensator built in. If the engine were rigidly mounted to the component being driven

(an electric generator, for example) this additional mass would need to be included. The example eight mass system shown here has eight ***degrees of freedom*** and eight ***natural frequencies***. The first three vibration ***modes*** are depicted in **Figure 16.27.** For each vibration mode the crankshaft will have that number of ***nodes*** – locations along the crankshaft at which angular deflection relative to the mean crankshaft speed is zero. Because crankshafts are relatively stiff only the first mode or two are generally of interest. As crankshaft stiffness increases the natural frequency of each mode increases; the natural frequencies of the higher modes of a crankshaft system are typically above the frequencies at which significant forces will be seen. It should be noted that for each vibration mode the ***anti-node***, or location of maximum angular displacement, is at the crankshaft nose. This results directly from the flywheel location at the opposite end of the crankshaft.

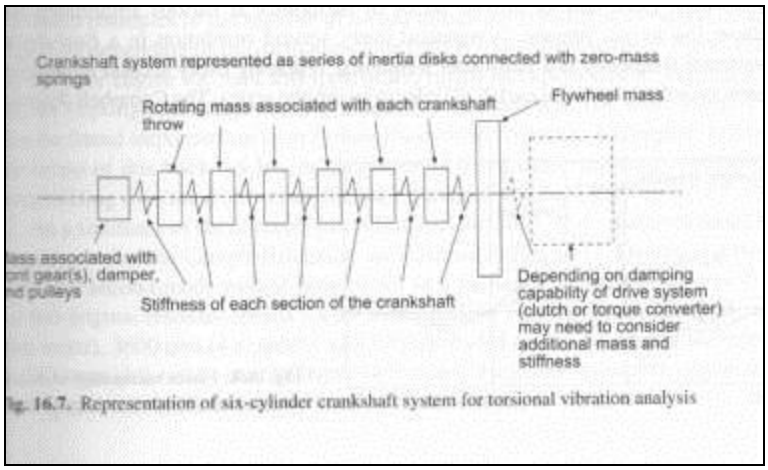

Figure 16.26: Representation of a…

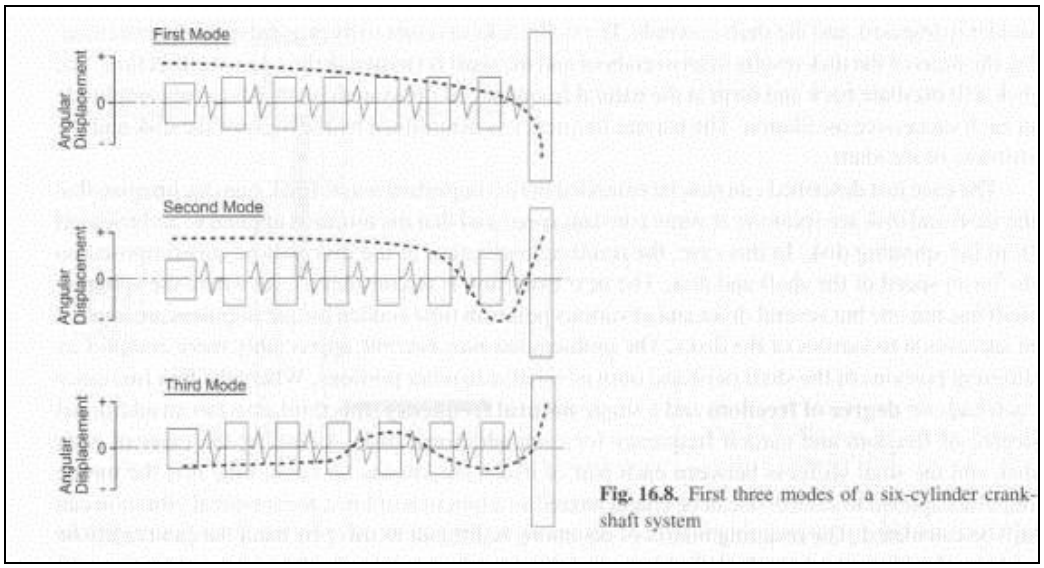

Figure 16.27: First three modes…

It is now important to look at the exciting forces – the net torque impulse applied at each crankshaft throw, or at each of the disks two through seven in the model shown in

Figure 16.26. The net torque impulse, as a function of crank angle is the net result of the pressure and reciprocating forces, as depicted in **Figure 16.28.** Because this combination of forces cannot be directly represented mathematically it is helpful to represent it as a Fourier Series. The torque signal is expressed as the sum of a constant value and an infinite series of harmonics at various amplitudes and frequencies. Because the torque impulse is repeated every second revolution in a four-stroke engine the fundamental frequency is a half-order frequency, repeating every second revolution. The remaining harmonics then represent each half order in an infinite series. The Campbell Diagram shown in **Figure 16.29** shows the frequency of each harmonic, from the half-order through the sixth order, as a function of engine speed.

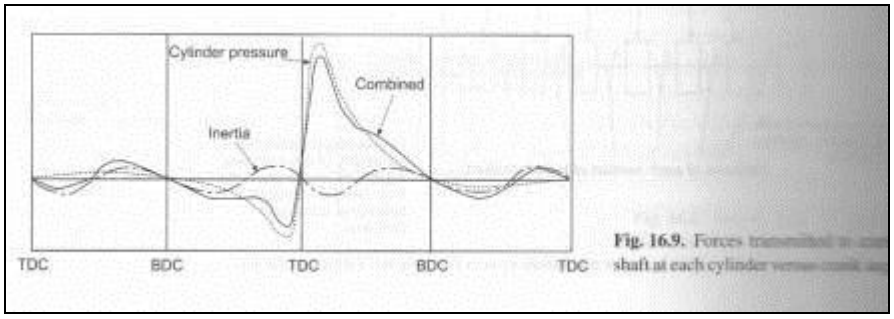

Figure 16.28: Forces transmitted…

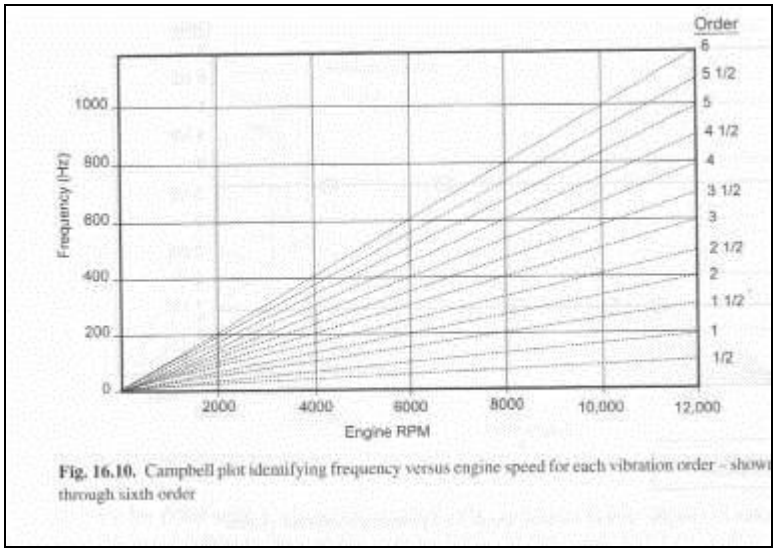

Figure 16.29: Campbell plot…

Torsional vibration requires the application of the torque impulse, now represented as a series of harmonics, to the crankshaft system described earlier. Returning to the Campbell Diagram (**Figure 16.29**) a given crankshaft will have various natural frequencies – one for each vibration mode described earlier. Each natural frequency can be overlaid as a horizontal line on the Campbell Diagram. It follows that there will be a critical, or resonant speed for every whole and half-order harmonic. Some of these will occur well outside of the operating speed range of the engine.

The torque impulses are being applied at various points along the length of the crankshaft, and in a particular sequence based on the engine's firing order. As a result some harmonic orders assist one another and increase the vibration amplitude. These are referred to as the ***major orders***. Others partially cancel one another and are termed ***minor orders***. The major orders tend to be those that are direct multiples of the number of torque pulses per revolution. However, other orders may be important depending on the particular crankshaft layout and firing order. For example, on an in-line six-cylinder engine the third and sixth orders might be expected to be important. The ninth order may be important although the magnitude of vibration is typically much lower. The 4 ½ order will also be found important on most in-line six-cylinder engines. A complete explanation is beyond the scope of this book, but lies in the choice of firing order resulting in relative high amplitude forces acting over the front versus the back halves of the crankshaft at the 4 ½ order.

As a summary of the concepts just discussed, the third, 4½, sixth, and ninth order frequency versus engine speed of the Campbell Diagram are re-plotted in **Figure 16.30**. Overlaid on this diagram are the first- and second-mode natural frequencies of a particular crankshaft system. It can be seen that for this engine resonant speeds for the first vibration mode will occur at approximately 2700 rpm (6th order), 3600 rpm (4 ½ order), and 5700 rpm (3rd order). Second mode resonance will occur at 7300 rpm (6th order) and 9600 rpm (4½ order). Note that unless the engine will be run at very high speed the third crankshaft vibration mode will not be seen.

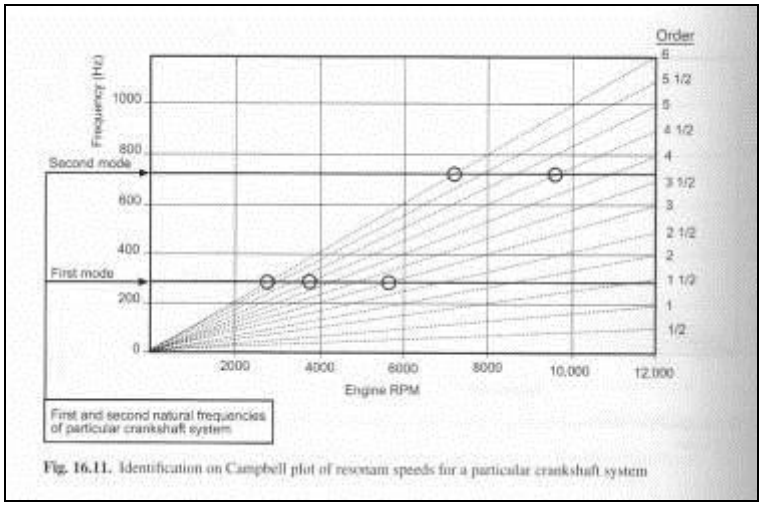

Figure 16.30: Identification on campbell…

Some general trends can be observed in crankshaft geometry. Higher stiffness crankshafts have higher natural frequencies which is important for both torsional stresses and lateral (axial) vibrations. Low moment of inertial cranks also help raise the natural frequencies of system. Conversely, adding counterweights adds to the moment of inertia of a crankshaft, lowering the frequency. On multi-throw cranks, such as V-6's or V-8's, shaping of the counterweights is critical to keep the $W*R^2$ low (inertia) and the W*R high (counterweight effectiveness).

For the reasons discussed at the beginning of this section dampening is applied to reduce the torsional vibration amplitude in most automotive engines. Various dampening

techniques can be used but the most common are the untuned viscous shear dampener and the tuned harmonic dampener.

A cross-section of a typical viscous shear dampener is depicted in **Figure 16.31** along with its effect on crankshaft deflection. The viscous shear dampener consists of a ring of mass encased in a cavity filled with a silicon-based fluid. The casing is rigidly bolted to the crankshaft nose, and the mass is free to float in the viscous fluid. As the crankshaft nose experiences a vibration impulse the mass reacts in the opposite direction, creating a shear force in the fluid that dampens the vibration impulse. The vibration energy is dissipated as heat energy from the viscous shear. This type of dampener is referred to as untuned because it will dampen the vibration pulses regardless of frequency, as can be seen in the plot of **Figure 16.31.** The unit must be sized large enough to dissipate the vibration energy without overheating, and adequate air flow around the dampener must be ensured. This type of dampener is relatively expensive so is generally seen only on larger, higher cost engines. Because the running clearance is quite small it is susceptible to damage.

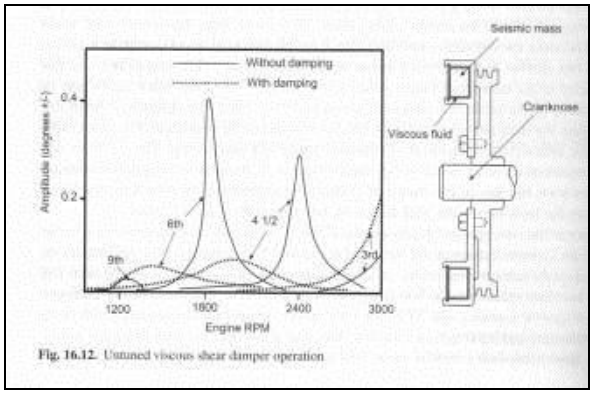

Figure 16.31: Untuned version…

More commonly used in automobiles is the tuned harmonic dampener shown in **Figure 16.32**. In this design the dampener hub is again rigidly mounted to the crankshaft nose, and a seismic mass is then mounted around the hub through a rubber isolator. The combination of the mass and the stiffness of the rubber isolator is tuned to dampen out vibration at a particular frequency, as shown in the figure. It should be noted that each order now has two resonant frequencies because the coupled mass acts as a second torsional system linked through the rubber isolator.

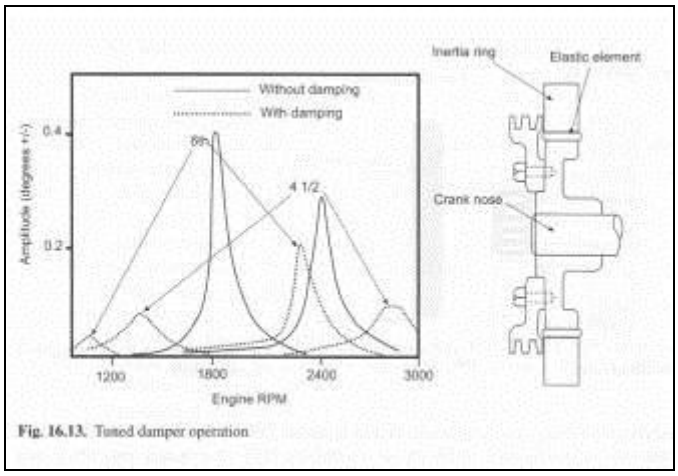

Figure 16.32: Tuned damper operation…

16.4.4 Crankshaft Nose Development (straight, taper, spline fit)

A cross-section showing an example of the crankshaft nose and the front details of the engine are shown in **Figure 16.33**. A cam drive gear is fit onto the front of the crankshaft and located using a keyway or spline. From this gear the camshaft will be driven using a gear, chain, or belt drive, as discussed further in Chapter 17. This or an adjacent gear may also be used to drive the oil pump and other internal engine drives (balancer shafts or a fuel pump are examples). The crankshaft nose then protrudes through the front cover, and the vibration dampener and accessory drive pulleys are mounted to the nose. The front oil seal is mounted to the front cover, and either directly contacts the crankshaft surface inboard of the dampener, or contacts the dampener hub as shown in the figure.

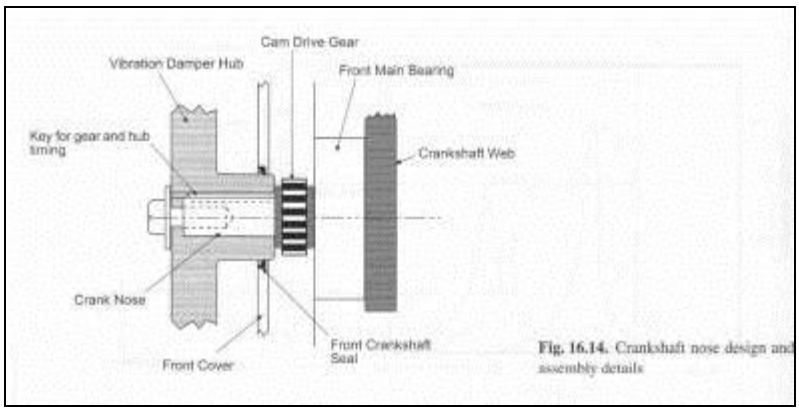

Figure 16.33: Crankshaft nose design…

There are three drive options for accessories at the front of the crankshaft: straight fit, taper fit, or spline. The torque capacity of each these joints need to be calculated to ensure a successful design. The straight fit and taper fit configurations will need a keyway, not to handle drive torque, but to ensure timing of the accessories to the

crankshaft. The torque applied to the clamping fastener(s) provides normal force and friction in the joint, which provides the torque capacity.

The objective of the straight fit joint is to design sufficient fastener clampload to withstand torsional loading on the crankshaft. Clampload is calculated by dividing the fastener torque by the nut factor of the joint and the diameter of the fastener as shown in **Equation 16.5**. Nut factors for steel joints are typically 0.18-0.22, but there is considerable variation in actual practice and this formula is an approximation for initial sizing purposes. Each of the input values has a tolerance and the nut factor (k) is sensitive to over 200 variables, which can affect final values significantly. It is best to design prototypes, and then validate the actual nut factor experimentally.

$$T_f = k \cdot F_{clamp} \cdot d \quad \text{or} \quad F_{clamp} = \frac{T_f}{k \cdot d} \tag{16.5}$$

Where:

F_{clamp} = Fastener clampload on hub
T_f = Fastener torque
k = Nut factor (described in Chapter 14)
d = Fastener nominal diameter

The fastener clampload provides the normal force on the joint, which is then multiplied by the coefficient of friction of the two components, the fastener and the hub. The resultant tangential friction force is multiplied by the maximum radius of the clamped members to calculate the torque capacity in the joint as calculated in **Equations 16.6-16.8** and illustrated in **Figure 16.34**. The torque capacity in the joint needs to be greater than the instantaneous torque expected on the crankshaft.

$$f = \mu \cdot F_{clamp}$$
$$T_j = f \cdot r$$
$$\frac{T_j}{T_i} > 1$$

(16.6) (16.7) (16.8)

Where:

μ = Coefficient of friction between hub and fastener, or hub and crank
f = Resultant tangential friction force
r = Maximum radius of the clamped members
T_j = Torque capacity in the joint
T_i = Instantaneous torque expected on the crankshaft

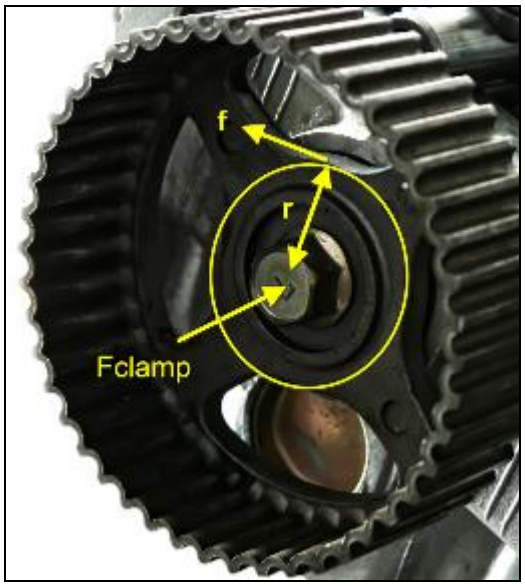

Figure 16.34: Summary of forces

The objective of the taper fit joint is again to provide sufficient fastener clampload (F_{clamp}) to withstand torsional loading on the crankshaft. However, the taper design is benefited by the interference fit generated between shaft and hub. These equations are developed from those used for a thick wall pressure vessel, and the variables are defined in **Figure 16.35**. This method assumes that the hub does not bottom against a shoulder, and is only supported by the taper. It also assumes that the clamping fastener does not bottom on the end surface of the shaft, to ensure that all fastener clamp force is going into the hub.

Calculate in the following order:

1. Contact Pressure
2. Maximum Introduction Force
3. Maximum Extraction Force
4. Maximum Torque Retention
5. Fastener Torque Specification

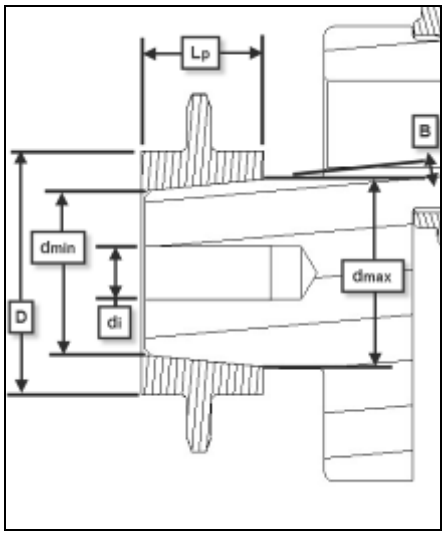

Figure 16.35: Taper Fit Variables

1. Use the assumed starting value for interference fit to calculate Contact Pressure as shown in **Equation 16.9**. Check to make sure yield strength of hub and shaft materials are not exceeded.

$$P = \frac{i}{\frac{d}{E_o}\left(\frac{1+ce^2}{1-ce^2}+\upsilon_o\right)+\frac{d}{E_s}\left(\frac{1+ci^2}{1-ci^2}-\upsilon_s\right)} \qquad (16.9)$$

$$d = \frac{d_{\min}+d_{\max}}{2} \qquad ce = \frac{d}{D} \qquad ci = \frac{d_i}{d}$$

Where:

P = Contact Pressure
i = Assumed interference fit
d = Mean Taper diameter
E_o = Young's Modulus of outer material (hub)
E_i = Young's Modulus of inner material (shaft)
ν_o = Poisson's Ratio for outer material
ν_i = Poisson's Ratio for inner material
c_e = Major diameter ratio
c_i = Minor diameter ratio
D = Outside hub diameter
d_i = Inner hole diameter

2. Use contact pressure to calculate Maximum Introduction Force required using **Equation 16.10**:

$$F_i = \pi \cdot d \cdot L_p \cdot P \cdot \left(f + \tan(\beta)\right) \quad (16.10)$$

Where:

L_p = Length of taper fit area
f = Coefficient of friction between components
β = Half of taper included angle

3. Use contact pressure to calculate Maximum Extraction Force for reference using **Equation 16.11**:

$$F_e = \pi \cdot d \cdot L_p \cdot P \cdot \left(f - \tan(\beta)\right) \quad (16.11)$$

4. Use Maximum Introduction Force to calculate Maximum Torque Retention by means of **Equation 16.12**, which is the maximum torque that the joint can withstand without spinning:

$$T_{\max} = F_i \cdot \frac{d}{2} \quad (16.12)$$

5. Now calculate the Fastener Torque required on the clamp screw with **Equation 16.13** to achieve introduction force calculated earlier, from the assumed interference fit. Check to make sure fastener load does not exceed material strength limits.

$$T_f = k \cdot F_i \cdot d_f \quad (16.13)$$

Where:

k = Nut factor, typically between 0.18-0.22 for steel
d_f = Fastener major diameter

If the calculated Fastener Torque required is higher than the actual value used to installed the hub to the taper, then the initial interference fit assumed is too high. Adjust the amount of assumed interference fit until the calculated Fastener Torque required equals the fastener torque actually applied. Then the amount of interference fit and torque retention is calculated correctly.

A splined joint can transmit more torque for its size than other types of joints as shown in **Figure 16.36-16.37**, and can be used at the nose of the crankshaft to drive accessory loads, or more commonly used at the power take off end of the crankshaft to drive the vehicle. Spline standards are published as ANSI B92.1 and ANSI B92.2m (metric). The objective of a spline is to drive using the teeth on the joint, and does not rely primarily on clamploat. Several failure modes must be designed for: base shaft breakage, hub bursting, teeth of spline shearing off at the pitch line, teeth of the internal spline breaking at root due to bending stress, and wear on the drive surface of the flank of the spline. Splines can be either “fixed”, where there is no relative or rocking motion

between the internal and external teeth as in a clamped joint, or "flexible" where there is relative rocking or axial motion. The following information was adapted from When Splines Need Stress Control by Darle W. Dudley, Product Engineering, 12/23/57. The equations presented below are for fixed splines, since they are most common in automotive application, and provide a nine times greater capacity for handling compressive stress than flexible splines.

Figure 16.36: Splined shaft

Figure 16.37: Splined hub (gear)

Calculate Torsional Shear Stress (S_{s1}) for the basic hollow shaft and design margin with load factors by applying **Equations 16.14-16.15**:

- The rated torque of an engine, usually found on a spec sheet, is the cycle averaged torque produced by the engine. In reality, the engine produces much higher instantaneous torque during peak cylinder pressure, and must be designed for.
- The Application Shock Factor (K_a) is typically high for internal combustion engines, as compared to turbines or an electric motor, because of this instantaneous torque. The fewer number of cylinders, the higher this number will be (2.8 for single or twin cylinder). The greater the number of cylinders, the more these instantaneous torque spikes will be averaged out (2.0 for 6 cylinders or more).
- The Fatigue Life Factor (L_f) will again be more severe for internal combustions engines as compared to turbines, because fully reverse loading will be experienced more often. A light duty automotive engine may experience comparatively few severe torque reversals, such as a hard launch-from-rest of the vehicle in first gear. A heavy duty truck engine may see many more torque reversals, as the engine is operated near its design limit for the majority of engine life.

$$S_{s1} = \frac{16 \cdot T \cdot D_{re}}{\pi\left(D_{re}^4 - D_{rh}^4\right)} \quad \text{and} \quad S'_{s1} > \frac{S_{s1} \cdot K_a}{L_f} \qquad (16.14)\ (16.15)$$

Where:

S_{s1} = Torsional shear stress of shaft
T = Peak instantaneous engine torque
D_{re} = Externally splined shaft, minor diameter
D_{rh} = Hole diameter of shaft, if present

S'_{s1} = Max allowable shear stress for material
K_a = Application shock factor (2.0-2.8 for IC engine)
L_f = Fatigue life factor
(1.0 for 10K cycles of light duty,
0.2 for 10M cycles of heavy duty)

Calculate Shear Stress in Spline Teeth at pitch diameter, and design margin with load factors via **Equations 16.16-16.17**:

- These equations can be modified to calculated shear stress in spline teeth at the root diameter of an external spline by substituting the minor diameter of the internal spline (Di) for the pitch diameter (D), and chordal thickness of the tooth at the minor diameter (t_x) for the thickness at the pitch diameter (t_c).
- The constant at the beginning of the equation can be modified depending on the quality of manufacture of the spline (4 if a less accurate means of manufacture are used, and 2 if a higher precision method is used).

$$S_{s2} = \frac{4 \cdot T \cdot K_m}{D \cdot N \cdot F_e \cdot t_c} \quad \text{and} \quad S'_{s2} > \frac{S_{s2} \cdot K_a}{L_f} \qquad (16.16)\ (16.17)$$

Where:
S_{s2} = Shear stress in spline teeth on shaft
constant = 4 assuming half of teeth carry load,
= 2 if all teeth carry load
K_m = Load distribution factor (1.0 for fixed splines, i.e. bolted joint with no relative movement)
D = Pitch diameter of splined shaft
N = Number of spline teeth on shaft
F_e = Face width of spline tooth, or axial length of spline engagement
t_c = chordal thickness at pitch line, or circular tooth thickness

Calculate compressive stress in spline teeth and design margin with load factors with **Equation 16.18-16.19**:

- Exceeding the compressive stress limits of the material will lead to fretting and premature wear, which leads to thinning of the teeth and shear failure.
- When splines may be exposed to an external environment outside of the engine, it is best to choose a more coarse pitch of teeth, so that any corrosion of the teeth reduces a smaller percentage of the tooth width over time than fine teeth.

$$S_c = \frac{2 \cdot T \cdot K_m}{D \cdot N \cdot F_e \cdot h} \quad \text{and} \quad S'_c > \frac{S_c \cdot K_a}{9 \cdot L_f} \qquad (16.18)\ (16.19)$$

Where:
S_c = Compressive stress in spline teeth on shaft
constant = 2, all teeth carry load after initial wear

F_e = Face width of spline tooth (1.0 * full face width for fixed spline)
h = radial height of tooth in contact
S'_c = Max allowable compressive stress for material

Calculate Burst Stress in Hub with internal spline teeth and design margin with load factors using **Equations 16.20-16.24**:

- Burst stress in hub is composed of a few types of loads: radial and tangential force components at the pitch line due to tooth profile, and centrifugal force of hub rotating at high speed.
- For engines, the stress due to centrifugal force is usually not significant unless the hub is of large diameter or the engine operates at high speeds.
- These stresses are summed and factors applied to determine final acceptable stress limits.

Bursting stress caused by the radial force component at the pitch line:

$$S_1 = \frac{T \cdot \tan\varphi}{\pi \cdot D \cdot t_w \cdot F} \qquad (16.20)$$

Where:
S_1 = Burst stress caused by radial force in hub
φ = Pressure angle of tooth
t_w = Radial wall thickness $(D_{oi} - D_{ri})/2$
D_{oi} = Outside dia. of internally splined hub
D_{ri} = Major dia. of internally splined hub
F = Full face width of hub

Bursting stress caused by centrifugal force (assume F < 1/3 * D):

$$S_2 = 0.828 \times 10^{-6} \cdot n^2 \cdot \left(2D_{oi}^2 + 0.424D_{ri}^2\right) \qquad (16.21)$$

Where:
S_2 = Burst stress caused by centrifugal force on hub
n = engine speed, RPM
D_{oi} = Outside dia. of internally splined hub, in.
D_{ri} = Major dia. of internally splined hub, in.

Tensile stress caused by the tangential force component at the pitch line:

$$S_3 = \frac{4 \cdot T}{D^2 \cdot F_e \cdot Y} \qquad (16.22)$$

Where:
S_3 = Tensile stress due to tangential force

Y = Lewis form factor (>1.5 for splines)

Total burst stress and Design margin:

$$S_t = K_a \cdot K_m \cdot (S_1 + S_3) + S_2 \quad \text{and} \quad S'_t > \frac{S_t}{L_f} \qquad (16.23)\ (16.24)$$

Where:

S_t = Total burst stress

S'_t = Max allowable tensile stress for material

The crankshaft nose is subject to high-cycle fatigue loading. The combination of the dampener and pulley mass and accessory drive belts create a resultant force of constant magnitude and direction. As the crankshaft spins each location on its nose experiences a complete bending load cycle once every revolution of the shaft. The outside surface of the nose experiences alternating tensile and compressive loads, and the threaded mounting hole(s) for the dampener assembly results in local stress concentrations, and the threads should be counterbored to mitigate. Rig testing can be readily devised to duplicate this load cycle and provide durability validation.

16.4.5 Crankshaft Flange Development

The same rationale just discussed for crankshaft nose loading and durability applies to the flywheel mounting flange as well. The flywheel or torque converter flex plate are typically mounted to the crankshaft flange using a multiple bolt pattern as shown in **Figure 16.38**. The flywheel connection relies on friction to generate the shear torque capacity in the joint, but a frictionless condition must also be designed for. To calculate the frictional torque capacity of the bolted joint:

1. Approximate nominal clampload per fastener
2. Calculate the shear capacity produced per fastener
3. Determine the total frictional torque capacity in the joint

Figure 16.38: Crankshaft flange bolted joint

1. Calculate the approximate nominal clampload per fastener with **Equation 16.25**, as covered previously:

$$T_f = k \cdot F_{clamp} \cdot d \quad \text{or} \quad F_{clamp} = \frac{T_f}{k \cdot d} \tag{16.25}$$

2. Calculate the shear capacity per fastener utilizing **Equation 16.26**:

$$F_s = \mu \cdot F_{clamp} \tag{16.26}$$

Where:

F_s = Force to slip the clamped joint at the individual fastener
μ = Friction coefficient, flywheel to crankshaft

3. Calculate the total frictional Torque Capacity in joint and Design margin via **Equations 16.27-16.28**:

$$T_c = F_s \cdot r_p \cdot n \quad \text{and} \quad \frac{T_c}{T} > 1.0 \tag{16.27) (16.28}$$

Where:

T_c = Frictional torque capacity in joint
r_p = Fastener pitch circle radius
n = Number of fasteners
T = Peak instantaneous engine torque

To calculate the <u>frictionless</u> shear capacity of the bolted joint:

4. Calculate the shear stress supported by half of the fasteners,

5. Calculate the shear stress on a single fastener or locating dowel.

For the first calculation, assume that half of the fasteners are loaded as the shank of the bolt contacts the clearance hole in the flywheel. Not all fasteners will share the load equally due to manufacturing tolerances, so a higher design margin of two or greater is recommended. The shear plane should go through the unthreaded shank of the bolt. If not, than the minimum diameter of the thread must be used in the calculation. However, it is generally good design practice to keep the fastener threads out of the shear region. For the second calculation, assume the entire load is taken up by a single fastener or a locating dowel, and that n = 1. A lower design margin of one or more is required since other fasteners will actually be loaded. It can sometimes be difficult to find the shear yield strength for fastener material, so as a first approximation, the distortion energy theory for ductile metals can be used.

4. Calculate the shear stress on the fastener(s) by means of **Equation 16.29**:

$$\tau_f = \frac{T}{r_p \cdot n \cdot A_f} \tag{16.29}$$

Where:

τ_f = Shear stress per fastener
T = Peak instantaneous engine torque
r_p = Fastener pitch circle radius
n = Number of fasteners
A_f = Cross sectional area per fastener

5. Calculate the Design margin via **Equation 16.30**:

$$\frac{\tau'}{\tau_f} > 2.0 \tag{16.30}$$

Where:

τ' = Max allowable shear stress for material
$\tau' = 0.58 * S'_t$ (distortion energy theory)
S'_t = Max allowable tensile yield

In order to increase the frictional torque capacity of the joint, it may be difficult to change the fastener pitch circle radius or fastener diameter once a design is in production. If it is desired to increase the fastener pitch circle diameter, the main journal diameter may need to increase. If the main journal diameter increases, it will increase the bearing diameter, seal diameter, cylinder block support web, and oil pan rail width, depending on design of the crankshaft.

It is a frequent occurrence that the marketing organization will request an increase in engine torque or power shortly after a new design is released to production. This is one key area of engine design to package protect for future increases in output!

If a design is complete and in production, and more torque capacity is required of the joint, various treatments can be added to increase the capacity of the joint at an additional cost. The coefficient of friction at the joint surface can be increase by changing the machined surface finish, by adding abrasive coatings, or by adding additional locating dowels. Alternately, the fastener grade may be increased to allow greater clampload.

Two examples of the rear crankshaft oil seal details are shown in **Figure 16.39** (update figure numbers). The case on the left incorporates a split seal in the rear main bearing. That on the right uses a continuous seal riding on the flywheel flange.

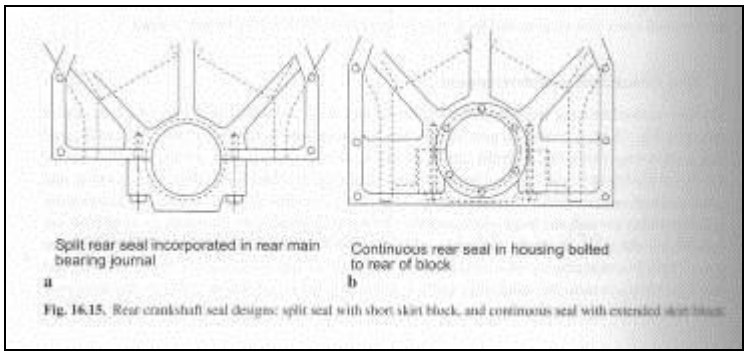

Figure 16.39: Rear crankshaft seal…

16.4.6 Cross-drilling of Crankshaft

Crankshafts are typically drilled for many reasons: material removal for balancing, material removal for weight reduction, and pressurized oil feed.

Crankshaft drilling for balance is usually done in the counterweight webs as shown in **Figure 16.40**. This is done when dimensions of the forging or casting of the base crankshaft cannot be held close enough to achieve the desired balance, or when a lighter piston is introduced that changes the required balance. This area is usually not significantly stressed, and so drilling does not present a significant stress concentration. These drillings can either be radial, as shown, to remove mass or can occasionally be axial in the same location to allow addition of more dense material such as tungsten alloy, depleted uranium, or lead. The addition of dense balance weights is more expensive, but can make the overall crankshaft lighter though a more efficient use of material (WR), or can be used to reduce crankshaft inertia for racing applications (WR^2).

Figure 16.40: Crankshaft drilling for balance, oil passages

Crankshaft drilling for weight reduction is typically done in the crankpin. This drilling of the crankpin reduces the amount of counterweight material required and can make the entire crankshaft lighter. It can also change the local stiffness of the crankpin, to better distribute stress in the crankshaft and reduce it in the critical journal fillet region. The crankpin is typically a highly loaded area, so attention must be paid to detailed design of the cross drilling in this area, and clearance in adjacent counterweights is typically required to allow access for this drilling. Frequently, this cross drilling is not coaxial to the crankpin.

If the crankshaft has plain bearings, it will be necessary to provide pressure lubrication via internal drilling of the crankshaft. These long drillings typically connect the main journal to the crankpin to provide pressurized lube and these internal drilled passages come very close the highly loaded crankpin and main journal fillets as illustrated in **Figures 1.6 and 1.8**. If the drilled passage comes close to the surface in a highly loaded area, either at a journal fillet or in the crank web, a fatigue crack may initiate. Additionally, care must be taken at the location where the drilled hole breaks the surface of the journal as this may also create a fatigue crack initiation point. The drilled oil hole is typically chamfered where it contacts the journal surface to diffuse stress, and also to spread pressurized oil to a larger area under the bearing. One technique to improve fatigue resistance is to use a hardened ball, and peen the ID of the chamfer where it meets the cross-drilled hole. This will introduce residual compressive stresses in this area and reduce a crack initiation site. Finally, the location where the oil hole breaks the surface of the crankpin is important for the bearings. It should be located somewhere between 90-30° BTDC compression stroke to provide the best feed of oil to the bearing. This is the point when the load on the bearing is least. Avoid the critical pressure region at 0-45° ATDC power stroke, when the high rod loading increases oil pressure above the system pressure, and blocks the feed to the bearings.

16.5 Detailed Design of Connecting Rod Geometry

The connecting rod is most likely the highest stressed component in the engine, and load is applied several times on every revolution of the engine. The connecting rod must be designed for high cycle fatigue to withstand the high number of engine cycles, and also for stiffness in supporting fluid film bearings. The connecting rod transfers the gas and inertia loads from the piston to the crankshaft, and experiences high rates of loading and direction reversal, high temperatures, and varying degrees of lubrication. Axial inertia and connecting rod whip forces (tangential to crank radius) are a function of connecting rod weight, so the higher the weight, the higher the forces. Since inertia can be a dominant load, and the piston, piston pin, and connecting rod all contribute, a more durable connecting rod design might require less material (be lighter) instead of the typical approach of adding more material to increase life. The higher the piston and rod weight, the more crank counterweight is required, which leads to a heavier engine. As a result, rod weight is of primary importance. Value added operations such as shot peening to enable a lighter connecting rod may be justified to reduce forces and weight in the rest of the powertrain. Piston normal forces due to connecting rod angle and connecting rod whip forces are translated to the engine, and require stronger support in the chassis. However, when a connecting rod fails, it typically destroys the entire engine similar to a crankshaft failure. The desire for minimum weight must be balanced with rod durability, and the desire for the least cost manufacturing methods. Connecting rods must also be cost effective, manufacturable, and serviceable.

The engine type has a significant effect on the highest loading. At one extreme is the low engine speed and high BMEP diesel, and at the other end is the high engine speed and lower BMEP gasoline engine. Gas loading and inertial loading at TDC oppose each other, reducing total loading on the connecting rod on the power stroke. At lower engine speeds, the gas forces dominate and put the connecting rod into compression. At higher engine speeds, inertial loads may dominate and stress the rod in both tensile and compression.

Connecting rod loads vary as a function of crankshaft angle, and also as a function of engine cycle. At TDC-exhaust (overlap) on a 4-stroke engine, the connecting rod experiences the highest tension load case because there are very little gas pressure forces to resist it. As opposed to TDC-Power stroke, when there will be a combination of tensile forces from inertia, and compressive forces from combustion. At BDC-exhaust, the inertia forces put the rod into compression.

The maximum tensile forces on the connecting rod occur at TDC-Exhaust as illustrated in **Equation 16.31**. Gas pressure forces can be neglected since they are near zero during valve overlap.

$$F_{recip,\,total} = -\left(m_{piston} + m_{conrod,\,recip}\right) \cdot r \cdot \omega^2 \cdot \left(\cos\theta + \lambda \cos 2\theta\right) \qquad \left(\lambda = \frac{r}{l}\right) \tag{16.31}$$

The maximum compressive forces on the connecting rod occur either at TDC-Power stroke for a low speed high BMEP engine, or at BDC-Exhaust for a high speed low BMEP engine as shown in **Equation 16.32**.

$$F_{recip,\,total} = -\left(m_{piston} + m_{conrod,\,recip}\right) \cdot r \cdot \omega^2 \cdot \left(\cos\theta + \lambda \cos 2\theta\right) - F_{Gas} \quad (16.32)$$

Notice that these equations are a function of the Connecting rod ratio (λ), **Equation 16.33**. As the connecting rod grows compared to the engine stroke, it has the tendency to reduce the peak force on the rod, and also the peak piston thrust force. However, a longer connecting rod has more weight and increases the engine deck height. These conflicting requirements must be balanced. Typical conrod ratios are:

$$\lambda = \frac{r}{L} \qquad \lambda \approx 0.20 - 0.35 \quad (16.33)$$

Where:

r = Crank radius, or stroke/2

L = Connecting rod length, pin to pin

The main beam of the connecting rod is subject to inertial bending forces (rod whip) as it swings through TDC. For an initial analysis, it is assumed that the connecting rod is a simply supported beam, subject to a linearly varying distributed load as shown in **Figure 16.41**. Once the connecting rod geometry is complete, FEA can be performed and the load can be spread to all of the elements of the beam in proportion to their distance from the piston pin end.

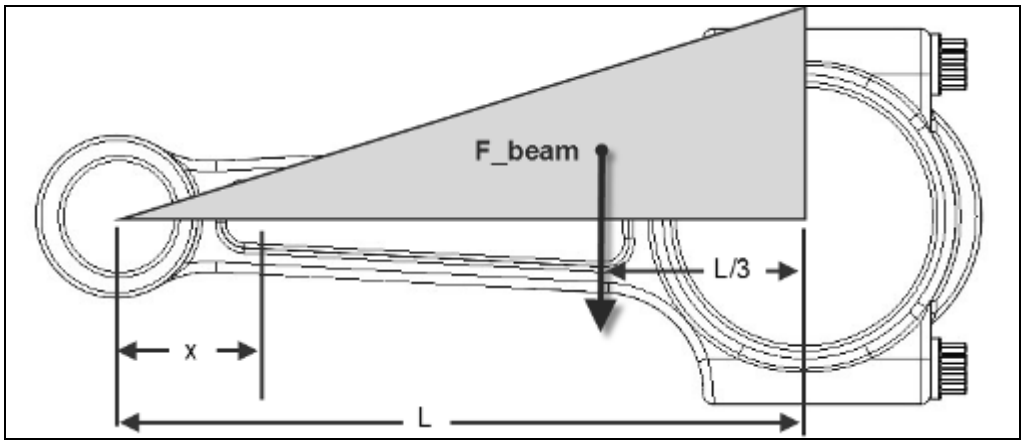

Figure 16.41: Simply supported beam with uniform increasing load

The total bending force due to the triangular distribution is found by using **Equation 16.34**:

$$F_{beam} = \frac{2}{3} \cdot m_{rod,upper} \cdot r \cdot \omega^2 \quad (16.34)$$

Where:

$m_{rod,\,upper}$ = Mass of connecting rod between two pins

The bending moment at a distance (x) from the piston pin end of the connecting rod is described by **Equation 16.35**:

$$M = F_{beam} \cdot \frac{x}{3} \cdot \left(1 - \frac{x^2}{L^2}\right) \tag{16.35}$$

The maximum bending moment occurs at x = L / √3, which simplifies to **Equation 16.36**:

$$M_{\max} = F_{beam} \cdot L \cdot 0.1283 \tag{16.36}$$

Since gas pressure loading dominates at low engine speed, the rod must be designed for compression. There is also a high compressive load at BDC due to inertia at high engine speed. In addition to designing for compressive stress, column buckling must also be considered and in high BMEP Diesel engines this is a very important consideration. The rod can buckle in one of two directions, parallel to the plane of connecting rod motion, and perpendicular to it as shown in **Figure 16.42-16.43**.

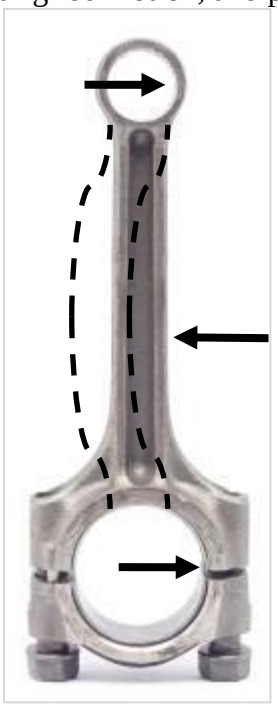

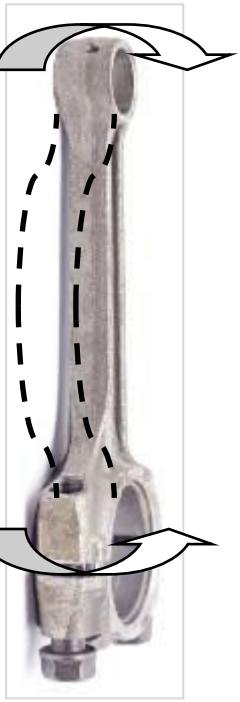

Figure 16.42: Buckling parallel to plane of motion
Figure 16.43: Buckling perpendicular to plane of motion

The end constraint on the connecting rod significantly influences its buckling resistance. If the rod is pinned at either end the least resistance to buckling is present, and if the rod is fixed in six degrees of freedom at either end the most resistance to buckling is present. Depending on the exact end constraint, the column is said to have an equivalent length (L_e) to a column pinned at both ends. Column buckling is also sensitive to the geometry of the cross-section, and it is assumed the connecting rod beam has a

constant cross section (if a tapered rod beam is present, proceed to FEA). The geometry is described by means of a slenderness ratio in **Equation 16.37**, which is the equivalent length of the column divided by the radius of gyration:

$$Slenderness\ Ratio = \frac{L_e}{\rho} \tag{16.37}$$

Where:

L_e = Equivalent length of the column
ρ = Radius of gyration

For the buckling condition parallel to the plane of connecting rod motion, the connecting rod is considered pined-pined or free-free, resulting in an equivalent column length of $L_e = 1.0L$. For the buckling condition perpendicular to the plan of connecting rod motion, the crankpin and piston pin limit rotation of the column at its constraints. This is a fixed-fixed condition and the equivalent column length is $L_e = 0.5L$

Now that the equivalent column length and slenderness ratio are defined, we may investigate the equations describing the critical compressive load which the column can sustain without becoming elastically unstable. First the compressive stress is evaluated, which is the maximum inertial force due to the piston and reciprocating portion of the rod mass, and the gas pressure force. The stress must be below yield in order for the column buckling formulas to be valid via **Equation 16.38**.

$$\sigma_{comp} = \frac{F}{A} \qquad \sigma_{comp} < \sigma_{yield} \tag{16.38}$$

Where:

F = Axial inertia force or gas force
A = Cross sectional area of beam

Next, either the Euler column buckling or J.B. Johnson Parabola method are used, depending on the slenderness ratio. While the axial compressive stress must be designed for fatigue resistance, the critical unit load of column buckling (S_{cr}) is a function of geometry and not material limits. The critical buckling stress at which the column becomes elastically unstable does not directly relate to yield or fatigue strength.

For columns with slenderness ratio $L_e/\rho > (2*\pi^2*E / S_y)\ ^{\wedge 1/2}$, use **Equations 16.39-16.40**:

$$F_{cr} = \frac{\pi^2 \cdot E \cdot I}{L_e^{\,2}}$$

$$S_{cr} = \frac{F_{cr}}{A} = \frac{\pi^2 \cdot E}{\left(L_e / \rho\right)^2} \qquad \text{(Euler)}$$

(16.39)(16.40)

Where:

L_e = Equivalent column length
ρ = Radius of gyration
E = Modulus of elasticity
S_y = Compressive yield strength
I = Moment of inertia
F_{cr} = Critical Load
S_{cr} = Critical Unit Load

For columns with slenderness ratio $L_e/\rho < (2*\pi^2*E / S_y)^{\wedge 1/2}$, use **Equation 16.41**:

$$S_{cr} = \frac{F_{cr}}{A} = S_y - \frac{S_y^2\left(L_e / \rho\right)^2}{4 \cdot \pi^2 \cdot E} \qquad \text{(J.B.Johnson)}$$

(16.41)

The actual compressive stress on the rod must be below the critical unit load S_{cr}. The graph in **Figure 16.44** depicts the various criteria: the compressive stress limit, the Euler Column buckling limit, and the J.B. Johnson Parabola limit.

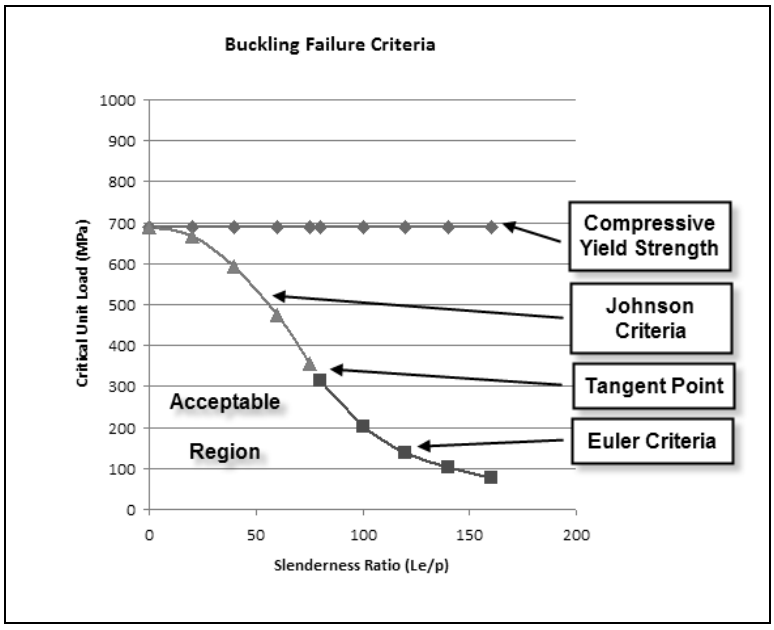

Figure 16.44: Graph of Buckling Failure Criteria

Euler and Johnson theories intersect at the tangent point, which is described by the **Equations 16.42-16.43** for X,Y coordinates. This tangent point distinguishes between long columns (Euler) and intermediate columns (Johnson).

$$S_{cr} = \frac{S_y}{2} \qquad \text{and} \qquad \frac{L_e}{\rho} = \sqrt{\frac{2 \cdot \pi^2 \cdot E}{S_y}} \tag{16.42)(16.43}$$

16.5.1 Connecting Rod Crankpin Bore Cylindricity

As we progress down the length of the connecting rod, different design criteria are required. The crankpin end of the connecting rod is primarily designed for stiffness and not strength, as the connecting rod needs to support the crankpin journal bearing and maintain roundness. As the engine progresses through its cycle, tensile inertia forces attempt to stretch the rod and deform the crankpin end of the connecting rod, as shown in **Figure 16.45**. Stretching of the connecting rod along the cylinder bore causes the connecting rod to pinch in along the cap split due to the Poisson effect, which may lead to the oil film breaking down and the bearing contacting the crankshaft. If rolling element bearings are used, pinching of the rolling elements may occur leading to skidding or spalling.

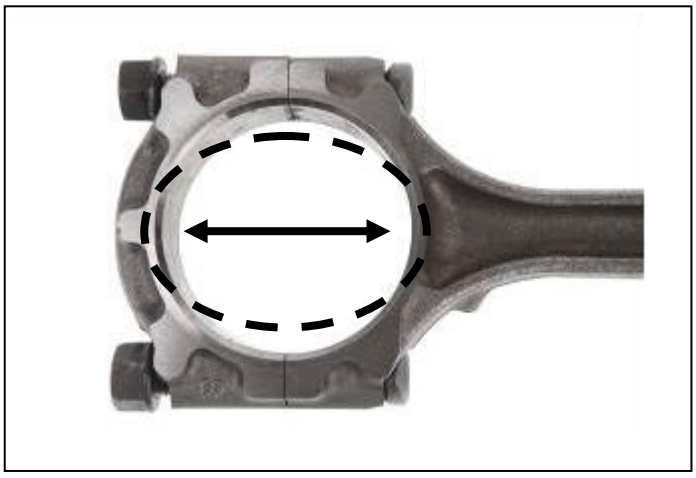

Figure 16.45: Deformed shape of crankpin bearing bore

Since downward compressive forces load the upper half of the bearing, and not the bottom half, only tensile forces are considered. Now, both the upper half and lower half of the rod mass are counted for inertial calculations. At TDC exhaust, the entire rod/piston system is creating a force away from the crank equal to the reciprocating force and the rotating force from the lower end of the rod as shown in **Equation 16.44**. This force is reacted by the lower end of the connecting rod. In high speed engines, this can

be the limiting load on the connecting rod because of ovalization of the crankpin bore, bolt limits, or cap strength.

$$F_{TDC-Exh} = -(m_{rot} + m_{recip}) \cdot r \cdot \omega^2 (1+\lambda) \tag{16.44}$$

Where:

m_{rot} = Rotating mass of connecting rod
m_{recip} = Reciprocating mass of connecting rod and piston assembly

In order to achieve a true deflected shape, the bearing press fit and support from the fluid film or rolling element bearing must be incorporated in this analysis. It is important to work with the bearing manufacturer to establish limits of cylindricity.

As can be derived from **Figure 16.45** above, the outer most surface of the split line has the largest stress. This is because as the rod cap is loaded in tension, the bolt flange will rotate about this outmost line of contact. As this line of contact is moved further away from the crankpin bore, the lever arm increases on the flange, and the unit load decreases. For this reason, most connecting rods have additional material added outboard of this flange to decrease unit loading and increase flange stiffness. Ideally the connecting rod bolt would be as close to the bore as possible, to reduce this flange rotation due to cantilever. A starting value for bolt diameter tied to cylinder bore diameter would be as shown in **Equation 16.45**:

$$D_{Fastener} \approx (0.1) \cdot D_{CylinderBore} \tag{16.45}$$

16.5.2 Connecting Rod-to-Cap Alignment

Connecting rod-to-cap alignment is critical to a successful rod design, and ensuring crankpin journal bearing life. Angular split lines present more of a challenge because of the direction of the applied forces in relation to the split line, but are sometimes necessary to aid in service of the engine in the vehicle.

Some alignment methods are:

- Increased Shank Fastener, increased shank diameter at split line, to provide alignment
- Ring Dowels, coaxial with the fastener in a counterbore, similar in function to increased shank fastener.
- Separate Dowel Pins, dowel pins next to the connecting rod bolt.
- Serration, specially machined rod-to-cap split surface.
- Stepped surface, specially machined rod-to-cap split surface.
- Cracked, manufactured by cracking the end of the rod off by force at either room temperature, or frozen.

Each method has pros and cons, which is why there are so many methods in use. The increased shank fastener is inexpensive to manufacture and is compact in design,

however if the alignment deviates from ideal there may be interference between the bolt and rod at the split line. This may add bending stress to the bolt, or upset material in the rod into the bearing bore and degrade circularity. Ring dowels are very similar in performance, with the added disadvantage of moving the rod bolt further away from the bearing bore. For packaging reasons, this may increase the overall rod size. Separate dowel pins are inexpensive, but may also increase the size of the connecting rod and add weight.

A serrated or stepped surface between the connecting rod and cap is more expensive to manufacture due to the increased sensitivity to manufacturing tolerances, but this type increases the shear resistance in the rod-to-cap joint. Stepped surface rod caps operate in a similar manner, using a lip to limit cap motion. Angle split rods increase the amount of shear force on the joint, and typically use these types of alignment.

The cracked design is used in high volume production, in both forged and powdered metal (PM) rods. This method is cheap, repeatable, insensitive to tolerances, and alignment and shear resistance are excellent. There is very low distortion of the split surface, since both surfaces are symmetrical. However this method dictates the parent material of the connecting rod, and may limit the choice of manufacturer since high production volumes are typically needed to justify the expense of special equipment to form and crack the rod.

16.5.3 Calculating Connecting Rod Bushing and Journal Bearing Press Fit

The small end, or pin end of the connecting rod is almost invariably a continuous bearing surface – no separation plane is needed as the piston pin can be inserted through the connecting rod from either side. Two designs are commonly seen for retaining the piston pin. One is the fixed pin, where the pin is pressed into the connecting rod bore, and rotates freely in the piston pin bore. The other is the floating pin, where the piston pin is free to rotate in both the piston and connecting rod bores, and is held in place with snap rings fitted in grooves on both outer edges of the piston pin bore. The fixed pin reduces cost and weight but has lower load carrying capability and requires special assembly provisions. The degree of required press fit generally requires the connecting rod to be heated. Because the connecting rod does not provide an acceptable bearing surface the floating pin requires the addition of a bushing to the connecting rod. This and the required snap rings and machined grooves significantly increases cost relative to the fixed pin. Traditionally the floating pin was seen only in high performance and heavy-duty engines, but due to the demand for increased loads it is now being adopted in many engines.

Interference fits are used to retain the piston pin bushing, as well as the crankpin journal bearing. Both are based on the same fundamentals of thick walled pressure vessels, but their application and assembly method are different. This requires different approaches to design. The thick wall pressure vessel equations are valid as long as the wall thickness-to-radius ratio is greater than 0.1.

Bearing press fits must be designed for operating loads, but also extremes of temperature. The goal is to have sufficient press fit to retain the bearing in its bore under

all operating conditions as presented in **Table 16.2**, while not exceeding the stress limits for the given materials. It may also be useful to use these equations to predict assembly press force at room temperature.

Table 16.2: Press conditions to evaluate

Tolerance (fit) \ Temperature	Maximum Temperature	Operating Temperature	Minimum Temperature
Maximum Interference	X		Y
Nominal Interference		X-Y	
Minimum Interference	Y		X

Depending on the material used for the housing and the material used for the bushing, differential thermal expansion may help or hurt the design. For a low thermal expansion coefficient housing (steel) and a high thermal expansion coefficient bushing (aluminum), the "X's" represent the extreme conditions to evaluate. For a high thermal expansion coefficient housing (aluminum) and a low thermal expansion coefficient bushing (steel), the "Y's" represent the extreme conditions to evaluate.

The minimum temperature conditions may exist while the vehicle is being stored, but not when the vehicle is being operated. So the minimum press fit retention may be violated if it is known that the vehicle will not be operated at these conditions. An example would be a motorcycle or lawn mower, which are not typically operated below 5°C, but may be stored in an unheated garage down to -30°C.

Figure 16.46 is an example of a representative automotive connecting rod, with input values listed in **Table 16.3-16.4**. This is a steel connecting rod with a Nickel-Aluminum-Bronze (C63000) bushing pressed in.

Figure 16.46: Connecting rod bushing

Table 16.3: Material properties for example

	Inner	Outer	
	C63000	**Steel**	
Modulus of Elasticity (E)	115	207	GPa
Poisson's Ratio (ν)	0.328	0.290	
Coef of Thermal Expansion (α)	16.2	13.0	μm/m-°C

Table 16.4: Input dimensions for example

Part Geometry		**Input Diameter**		**Input Radius**	
Inner	Inner	21.68	r_i =	10.84	mm
Member	Outer	24.58	r_o =	12.29	mm
Outer	Inner	24.54	r_i =	12.27	mm
Member	Outer	36.00	r_o =	18.00	mm

Press Fit Width (in) = 21.08
Friction Coefficient = 0.10

The steps used to calculate the stress in the pressed members are:

1. Check thick wall assumption is valid.
2. Assume a starting value of interference fit.
3. Calculate circumferential (hoop) stress and radial stress. Longitudinal stress assumed = 0 if members are the same length.
4. Calculate the diametral strain.
5. Solve for P, and calculate the fit pressure.

Check Thick Wall Assumption is Valid using **Equation 16.46**:

$$\frac{Wall\ Thickness}{Radius} \geq 0.1 \qquad \frac{(12.29 - 10.84mm)}{10.84mm} > 0.1 \qquad (16.46)$$

Assume a Starting Value of Interference Fit:

$$I_{Diametral} = x \qquad I_{Diametral} = 0.045mm \qquad (16.47)$$

Calculate circumferential (hoop) stress and radial stress for the Outer Cylinder via **Equations 16.48-16.49**:

$$\sigma_{c,i} = \frac{(r_o^2 + r_i^2)p}{(r_o^2 - r_i^2)} \qquad \sigma_{c,i} = \frac{(18.00^2 + 12.27^2 mm^2)p}{(18.00^2 - 12.27^2 mm^2)} = 2.74p$$

$$\sigma_{r,i} = -p \qquad \sigma_{r,i} = -p \qquad (16.48)(16.49)$$

Calculate the Diametral Strain for the Outer Cylinder by means of **Equations 16.50-16.51**:

$$\varepsilon_i = \frac{\sigma_{c,i} - \upsilon(\sigma_{r,i})}{E} \qquad \Delta d_{o,inner} = \varepsilon_i d_{i,outer}$$

$$\varepsilon_i = \frac{2.74p - 0.290(-p)}{207GPa} = 1.46\times10^{-5}\,p \qquad \Delta d_{o,inner} = (1.46\times10^{-5}\,p)(24.58mm) = 3.59\times10^{-4}\,p \quad (16.50)(16.51)$$

Calculate circumferential (hoop) stress and radial stress for the Inner Cylinder employing **Equations 16.52-16.53**:

$$\sigma_{c,o} = \frac{-(r_o^2 + r_i^2)p}{(r_o^2 - r_i^2)} \qquad \sigma_{r,o} = -p \qquad \sigma_{c,i} = \frac{-2r_o^2 p}{(r_o^2 - r_i^2)}$$

$$\sigma_{c,o} = \frac{-(12.29^2 + 10.84^2\,mm^2)p}{(12.29^2 - 10.84^2\,mm^2)} = -8.01p \qquad \sigma_{r,o} = -p \qquad \sigma_{c,i} = \frac{-2(12.29^2\,mm^2)p}{(12.29^2 - 10.84^2\,mm^2)} = -9.01p \quad (16.52)(16.53)$$

Calculate the Diametral Strain for the Inner Cylinder by utilizing **Equations 16.54-16.55**:

$$\varepsilon_o = \frac{\sigma_{c,o} - \upsilon(\sigma_{r,o})}{E} \qquad \Delta d_{i,outer} = \varepsilon_o d_{o,inner}$$

$$\varepsilon_o = \frac{-8.01p - 0.328(-p)}{115GPa} = -6.68\times10^{-5}\,p \qquad \Delta d_{i,outer} = (-6.68\times10^{-5}\,p)(24.54mm) = -1.64\times10^{-3}\,p \quad (16.54)(16.55)$$

Apply **Equation 16.56** to solve for P, and calculate the fit pressure:

$$I_{Diametral} = |\Delta d_{o,inner}| + |\Delta d_{i,outer}| \qquad 0.045mm = |3.59\times10^{-4}\,p| + |-1.64\times10^{-3}\,p| \qquad p = 22.5MPa \quad (16.56)$$

Use the distortion energy failure criterion for the limit of design, assuming ductile materials. The maximum stress for both the internal and external members occurs at their inner surfaces. To improve the accuracy of the final analysis for not circular components, apply FEA. Also, it is important to evaluate these same equations at the limits of the component tolerances, since a design may be acceptable at nominal tolerance, but not acceptable at a least material condition.

The maximum press force is determined by **Equation 16.57**:

$$F_{\max} = f\,N = 2\pi f\,p\,r_{shaft}L_{press} \quad (16.57)$$

$$F_{\max} = 2\pi(0.1)(22.5MPa)(12.29mm)(21.08mm) = 3660N$$

The maximum torque to spin is determined by **Equation 16.58**:

$$T_{\max} = 2\pi f p r_{shaft}^2 L_{press} \tag{16.58}$$

$$T_{\max} = 2\pi(0.1)(22.5MPa)(12.29^2 mm^2)(21.08mm) = 45.0 \text{ N} - \text{m}$$

As the temperature and size of the components change, so will the press fit. Every element of the material expands with increasing temperature, and each element moves outward from its original position, so a hole bored in a solid will increase in diameter. The math for this follows the equation for linear thermal expansion, and is applied to the circumference of the hole in **Equation 16.59**:

$$\begin{aligned} &\Delta L = \alpha L_o (T_2 - T_1) \\ &L_o = Circumference = 2\pi R \quad or \quad \pi D \\ &\Delta L = \alpha \pi D (T_2 - T_1) \end{aligned} \tag{16.59}$$

Where:

ΔL = Change in length of feature
α = Coefficient of linear expansion
L_o = Initial length of feature
T_1 = Initial temperature of component
T_2 = Final temperature of component

Through manipulation, a useful relationship can be derived for change in diameter due to temperature employing **Equations 16.60-16.62**:

$$\begin{aligned} &L_{original} + \Delta L = L_{New} \\ &\pi D_o + \alpha \pi D_o (T_2 - T_1) = \pi D_N \\ &D_o (1 + \alpha (T_2 - T_1)) = D_N \end{aligned} \tag{16.60) (16.61) (16.62}$$

Where:

D_o = Original diameter
D_N = New diameter

The final hoop stress on the crankpin end of the rod is developed in much the same way as the press fit bushing example above, except the bearing is split into two different pieces for installation in the upper rod and cap. The diameter of the journal bearing is slightly larger than the bore in the connecting rod (or main bearing), and is compressed during installation. Since the bearing is neither uniform in thickness, or constant in radius, a direct measurement of the diameter is misleading. A different

method of measurement is required to describe the press fit. This is called crush height and is measured by the overstand test, the amount of which affects the press fit. The overstand test consists of placing the bearing shell in a half circle gauge, flush at one end and extending above the other. The amount the shell protrudes from the gauge is the amount of circumferential crush the bearing will be under when assembled. A complete description of the overstand test is listed in:

- **ISO 3548:** Plain bearings — Thin-walled half bearings with or without flange — Tolerances, design features and methods of test.
- **ISO 6524:** Plain bearings — Thin-walled half bearings — Checking of peripheral length.

The crush height is measured under a gauge force. This is effectively measuring the circumference or length of the journal bearing shell, rather than diameter. A bearing with sufficient crush height ensures that the bearing is preloaded enough to have uniform contact with the housing. This ensures good heat transfer from the bearing to the housing, and prevents fretting. Typical values of the crush height of automotive bearings are 0.05-0.10mm.

The theoretical basis for calculating the bearing crush is a thick column in compression, applying **Equation 16.63**. This column is curved into a shell. Column buckling can be ignored since the bearing is supported by the housing in the installed state.

$$Crush\ Height = \Delta = \frac{PL}{A_b E} \tag{16.63}$$

Where:

P = Gauge force
L = Length of shell bearing (in circumference direction)
A_b = Cross sectional area of bearing
E = Modulus of elasticity of bearing

Next the circumferential length for the shell is calculated, and substituted into the original formula as represented by **Equation 16.64**:

$$L = \frac{\pi D}{2} \qquad \Delta = \frac{P\pi D}{2A_b E} \tag{16.64}$$

Then the spring rate is calculated using **Equation 16.65**, and rearranged into a useful ratio for visualization, called the Deflection Rate (DR):

$$k = \frac{P}{\Delta} = \frac{2A_b E}{\pi D}$$
$$DR = \frac{k}{A_b} \times 10^{-4} \tag{16.65}$$

The spring rate can now be used to calculate compressive stress with **Equation 16.66** in the bearing shell:

$$\sigma_{comp} = \frac{P}{A_b} = \frac{k\Delta}{A_b} \tag{16.66}$$

Now, to calculate the circumferential stress in the connecting rod around the bearing, use **Equations 16.67-16.68** to determine the minimum developed length and the maximum developed length of the bearing shell:

$$Minimum = L_1 = \frac{\pi D_1}{2} \tag{16.67}$$

$$Maximum = L_2 = \left(\frac{\pi D_2}{2}\right) + \left(2 \cdot H_G\right) + T_G - D_2 \tag{16.68}$$

Where:

D_1 = Housing bore diameter, minimum
D_2 = Housing bore diameter, maximum
H_G = Gauge height, or depth of half circle in block, sometimes referred to Q/2
T_G = Crush height, height bearing shell protrudes from gauge block

Using the developed lengths, the stress can now be calculated with **Equation 16.69**. As with the piston pin bushing, the stress must be evaluated at extremes of temperature and tolerance if dissimilar materials are used.

$$\sigma = \frac{\left(L_2 - L_1\right)\left(\frac{E_L \cdot A_b}{L_2}\right) + F_G}{A_r} \tag{16.69}$$

Where:

σ = Circumferential stress in connecting rod at minimum cross section
E_L = Modulus of Elasticity of journal bearing shell
F_G = Gauge checking load
A_r = Minimum cross sectional area of connecting rod

16.5.4 Typical Connecting Rod Computer Stress Analysis Methodology

Typically, the entire connecting rod is not analyzed. A half model with symmetry, or even a quarter model, is used. The mesh is typically refined around the bolted joint area, and around critical fillets and transitions. The connecting rod is analyzed in the following steps.

Apply the assembly load cases by applying the bolt preload to the connecting rod cap. Incorporate the deformations into the initial geometry of the model to simulate machining of the crankpin bore when clamped together. Apply the bushing and bearing assembly load cases by simulating the interference due to press fit of piston pin bushing and crankpin journal bearings.

Analyze the dynamic load cases produced by the engine by applying maximum tensile load at TDC-Exhaust stroke and maximum compressive at BDC-Power stroke. The piston pin and crankpin are modeled as separate cylinders and used as boundary conditions since they contribute to the overall system stiffness. Finally, analyze loading due to rod whip.

The last step of the analysis is to evaluate the connecting rod for critical column buckling in the plane of connecting rod motion, and perpendicular to it. This enables a more refined solution to the analytical method, since detailed geometry is represented.

16.6 Detailed Design of Flywheel Geometry

The purpose of the engine flywheel is to smooth the cyclical speed variation of the engine within a given engine revolution. It absorbs energy during the power stroke, and distributes it during the exhaust, intake, and compression strokes. The transmission of instantaneous torque spikes developed by the engine will be reduced to the driveline.

The flywheel or torque converter mass is important in controlling idle speed fluctuation within limits acceptable to the driver. As speed increases fluctuations become much less apparent and the need for this mass decreases. An acceptable idle speed fluctuation limit is identified and flywheel mass is chosen to be sufficient to reduce fluctuation within that limit. Additional mass beyond the minimum required will penalize the engine's response to transient requirements.

This storage and release of energy has other uses in the engine and the vehicle, when the engine average speed changes. Large flywheel inertia will enable a low engine idle speed. A low engine idle speed, by reducing the total number of revolutions the engine makes at idle, will reduce fuel consumption and improve emissions during an engine operating regime that does little useful work. The lower the speed variation, the easier it is to calibrate the fuel injection at low engine speeds as the piston approach to TDC is more consistent.

Like in heavy machinery, the flywheel will allow sudden loads to be placed on the engine without stalling it. This is helpful when starting a vehicle from rest, or during sudden load changes. The inertia of the flywheel can be balanced against the inertia of the vehicle. A large engine flywheel will also make the engine less responsive during transient drive modes, as the engine will not accelerate quickly with the application of throttle and will not decelerate quickly during coasting/sail or removal of the throttle. This may have a beneficial affect in a work truck or for cruising on the highway at steady speeds, but may not be desirable in a sports car where quick engine response is desired.

Additionally, in most applications, it serves as the power take off location and usually as a means for the starter drive of the engine.

In many cases the flywheel and crankshaft are balanced as a unit, and a non-symmetric bolt circle or locating dowel is used to ensure that if the flywheel is removed it is again mounted in the same position. The clutch disc and pressure plate are then mounted to the flywheel with a series of cap screws around the perimeter of the pressure plate. A pilot bearing or bushing mounted in the rear of the crankshaft at the shaft centerline supports the nose of the transmission input shaft. In transverse installations this shaft may not feed directly into the transmission, but drives a chain that then transfers load to the transmission.

In the case of an automatic transmission a flex plate, bolted to the same bolt circle on the crankshaft flange, replaces the flywheel. The torque converter is then bolted to the flex plate with three or four bolts near its perimeter.

16.6.1 Calculating Flywheel Inertia Effect on Cyclical Speed, Energy Storage

Equation 16.70 for Kinetic Energy stored in a flywheel is shown below, and is equivalent to the amount of energy release if the flywheel speed changed from current to a full stop:

$$E = \frac{I\omega^2}{2} \quad or \quad \frac{Wv^2}{2g} \tag{16.70}$$

Where:

E = Energy stored in the flywheel
I = Polar moment of inertia
ω = Rotational velocity
W = Weight of flywheel rim
v = Linear velocity at mean radius

Typically, a flywheel is designed to reduce the speed fluctuation to a desired amount. This is measured in percent change in speed called the Coefficient of Fluctuation (C_f) as represented in **Equation 16.71**, or in absolute speed change. For engines, this is typically between 2-5%. If a lower speed fluctuation is desired, a larger flywheel will be required. However, the larger the flywheel, the more difficult to package and the heavier the engine will be. Since the flywheel is usually directly coupled to the crankshaft, it is not possible to spin the flywheel faster than engine speed, removing this as a design option. To gain smoothness, the flywheel diameter or thickness will need to be increased. Generally $I \sim mr^2$, so a thin disc of large diameter would have most efficient use of material, and a hub with most material concentrated near the rim would be even better. Typically dense materials such as steel or cast iron are used for flywheels.

$$C_f = \left| \frac{\omega_2 - \omega_1}{\omega_{mean}} \right| \tag{16.71}$$

If the velocity of a flywheel changes, the energy it absorbs or discharges will be proportional to the difference of initial and final speeds per **Equation 16.72**:

$$E = \frac{I\left(\omega_2^2 - \omega_1^2\right)}{2} \quad or \quad \frac{W\left(v_2^2 - v_1^2\right)}{2g} \tag{16.72}$$

The traditional method for calculating the required amount of energy in the flywheel is to determine the peak energy needed by the work operation and subtract the average energy provided by the engine or motor providing energy input, and the difference is the flywheel energy needed to maintain speed as represented in **Equation 16.78**. This method is relevant to the vehicle side, as a load is applied to the vehicle, the required flywheel inertia to maintain engine speed can be calculated.

$$E_{work} - E_{motor} = E_{Flywheel} \tag{16.78}$$

Once the desired flywheel energy storage is determined, and the desired speed fluctuation is set, the equation can be rearranged to determine inertia required utilizing **Equation 16.79**:

$$I = \frac{2E}{\left(\omega_2^2 - \omega_1^2\right)} \tag{16.79}$$

Once the required polar moment of inertia is determined, **Equation 16.80** for a hollow cylinder or ring can be used to determine the required diameter and length.

$$I = \frac{\pi\left(d_o^4 - d_i^4\right)}{32} \cdot L \cdot \rho \tag{16.80}$$

Where:

d = Outer and inner diameter of hub
L = Length or width of hub
ρ = Density of material

16.6.2 Calculating Burst Strength of Flywheels

The design limit of flywheels varies by geometry, material, and speed of flywheel. Assuming the flywheel is a hub or hollow cylinder as illustrated in **Figure**

16.47, maximum tangential and maximum radial stress can be calculated using **Equations 16.81-16.82**. The maximum tangential stress will occur at the inner diameter, and the maximum radial stress will occur at the geometric mean radius, $\sqrt{(r_o r_i)}$.

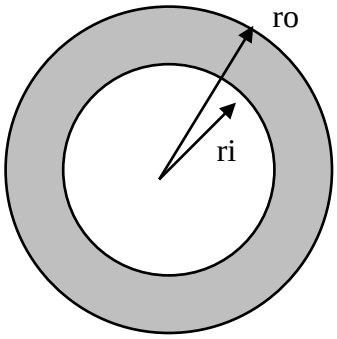

Figure 16.47: Illustration of flywheel dimensions

$$\sigma_{t,\max} = \left(\frac{\rho\omega^2}{4}\right)\left((3+\upsilon)r_o^2 + (1-\upsilon)r_i^2\right) \tag{16.81}$$

$$\sigma_{r,\max} = \left(\frac{3+\upsilon}{8}\right)\rho\omega^2\left(r_o - r_i\right)^2 \tag{16.82}$$

Where:

ν = Poisson Ratio
r_o = Outer radius of hub
r_i = Inner radius of hub

16.6.3 Calculating Critical Speeds of Shafts or Whirl of Flywheels

If the engine is to be used in a configuration where the crankshaft and transmission input shaft are not co-axial, in other words where the crankshaft and transmission input shaft are connected by a gear pair, the critical speed of the shaft under radial load must be considered. This is different than the critical speed under torsional load. All rotating shafts have a slight imbalance, and at a critical speed the flywheel no longer rotates about its geometric axis but about the true center of gravity, known as whirl. Critical speeds of shafts are outside the scope of this book, but must be considered in detailed design and analysis.

Considering weight, speed, and energy are contained in a flywheel. It is typical practice to utilize higher design margins when designing a flywheel. It is also important to evaluate the sensitivity of the stress to various input parameters. A lower design

margin can be used for material properties, since the relationship is linear, however speed is a function squared so the design margin is more sensitive to this parameter.

16.7 Crankshaft and Connecting Rod Construction

16.7.1 Crankshaft Materials

Crankshafts are typically cast or forged out of iron or steel. Many types of cast iron are used from gray iron, to malleable iron, to nodular iron. The classic tradeoff is one of cost versus strength. Typically cast gray iron would be used for low output engines such as lawn care, while high output engines such as race cars or diesel trucks would use forged steel. For low volume production, crankshafts are occasionally machined from steel billets, but this is the most expensive manufacturing method due to long machining times.

Crankshaft steels are typically medium carbon (.3-.4 percent) and heat treated to 125-150 ksi tensile strength. Forged crankshafts have better material strength due to grain flow. Cast iron alloys vary over a wide range from 30-120 ksi tensile strength depending on material and heat treat, and their values can be found in many references.

While the merits of cast versus forged can be compared, component geometry often dictates the method chosen. It is easier to forge a crankshaft that has all of its crankpins in the same plane, such as a single-cylinder or inline-four cylinder, because this allows a simple open and shut die. Cross-plane crankshafts such as **Figure 16.48** can be forged, but more material removal is often required. A cast crankshaft can more easily handle a cross-plane crank geometry while reducing the total amount of machine stock removal required.

Casting a crankshaft can enable other desirable geometry for little cost, such as hollow crankpins and detailed shaping of the counterweight webs. The development of the metallurgy and casting methods has allowed the use of cast cranks in more and more applications. Where packaging dimensions are not strictly constrained, cast crankshafts can be a reasonable alternative to forged steel shafts.

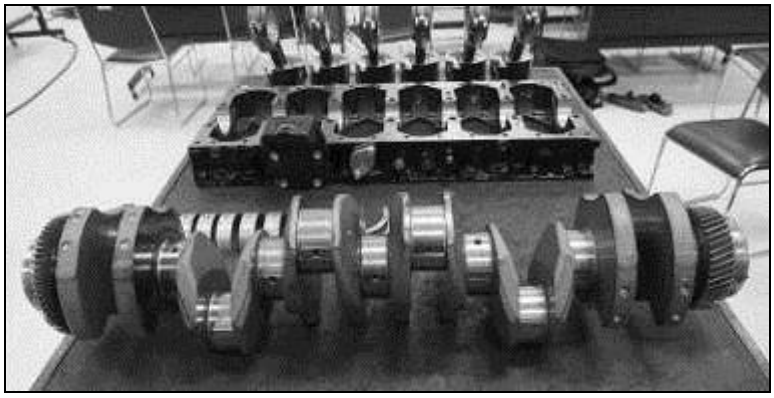

Figure 16.48: One piece crankshaft, forged, machined

Directly consult a casting or forging supplier for custom alloys, heat treat options, and local geometry properties. This is a changing field influencing crankshaft design, and is an area where the state of the art in crankshaft design is developing.

16.7.2 Crankshaft Manufacturing

Crankshafts are usually manufactured through several operations. They proceed from casting or forging, to rough machining, to finish machining, to grinding, to polishing. Depending on the material chosen or application, heat treat processes may be involved and additional value added operations may be employed.

The direction of rotation in the engine is important to the grinding and polishing operations if plain journal bearings are used. When the grinding operation is performed on the crankpin and main journal surfaces, the metal removal process smears the material at the surface. This smearing of the metal raises small burrs or whiskers as shown in **Figure 16.49**, and can be thought of as a circular saw blade in cross section. If these whiskers remain on the finished crank, they will have a tendency to scrape the bearings on startup, and lead to premature wear. This is important during solid lubrication and mixed lubrication at engine startup, prior to the development of the full oil film. Therefore it is important to specify the direction of rotation on the crankshaft drawing. The bearing journals are ground opposite to rotation direction, and polishing is done in the direction of rotation, to encourage the whiskers to fold down upon rotation.

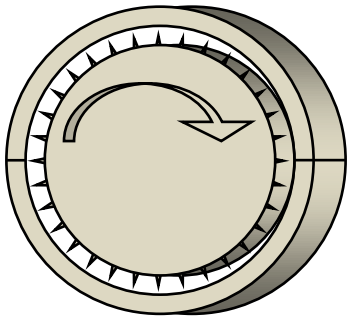

Figure 16.49: Illustration of burrs on shaft

An additional consideration in the design of crankshafts is access for the journal grinding wheel. This grinding wheel is often many times the diameter of the crankpin, to allow unobstructed access to the journal bearings, but still clearance can become a limitation. In addition to clearance for the journal bearings, access may be needed to manufacture splines or timing gears made integral to the shaft.

Finally, for extreme applications or applications where the loading will be increased on an existing engine design, steps may be taken to increase crankshaft strength in the critical fillet transitions. These value added operations are ion nitriding, shot peening, induction hardening, and fillet rolling or roll hardening as summarized in **Figure 16.50**. These operations locally increase the strength of the crankshaft by modifying the material properties or introducing compressive residual stresses. These additional

operations cost additional money, and careful design can often avoid their requirement. However, the designer must compare added cost to processing of the crankshaft, to the larger implications to the engine and vehicle downstream. In order to increase the power output of the engine, these processes can be added without having to redesign the engine. Enabling smaller journal diameters can reduce engine friction. These operations can be beneficial when considering the system as a whole.

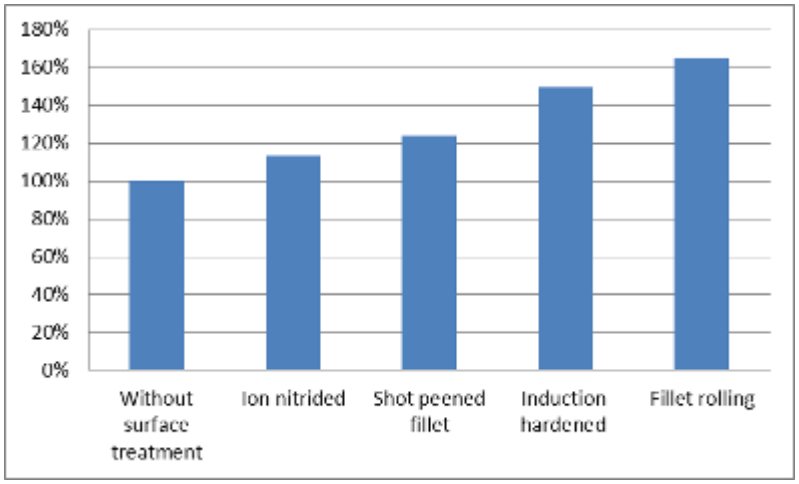

Figure 16.50: Comparison of metal improvement techniques

16.7.3 Connecting Rod Materials

Several different materials and processes are used to make connecting rods. Historically rods have been cast, forged, or machined from billet. Recently, connecting rods have been manufactured from forged powdered metal (PM) for high volume automotive applications. This process can be lower cost, enabling more consistent parts and a beneficial rod cap alignment surface. Heavy duty engines still primarily use forgings.

The materials used are cast iron, steel, aluminum, and titanium. Cast iron is typically used in cost sensitive applications, with forged steel being used in high load applications. Aluminum connecting rods are being used in light duty engine applications, and recent improvements in metallurgy have increased the suitability of this material. Recall from above that the connecting rods own weight acts against itself in high RPM applications, so lighter materials enable higher RPM. Expensive Titanium is typically reserved for racing applications, due to cost.

16.7.4 Connecting Rod Manufacturing

Connecting rods are typically manufactured using several steps. They proceed from casting or forging, to rough machining of the upper rod and rod cap separately.

These two components are then bolted together for the finish machining of the assembly and precision honing of the bores. It is important to perform this precision machining in the assembled state, as bolt clamp loads will distort the big end bearing shape, and cylindricity is key to fluid film bearing life. Occasionally, the piston pin bushing and crankpin journal bearing are assemble to the rod, and an additional boring and honing operation is performed if a higher class of tolerance is to be maintained.

Frequently, value added operations are applied to the connecting rod to increase component life, or reduce component weight. Trimming of a casting or forged connecting rod blank will often leave score marks in the finished part. These score marks can act as stress risers in the key loaded areas of the connecting rod. They may be ground or polished smooth to reduce the stress concentrations. Additionally, shot peening of the connecting rod will introduce compressive residual stresses in the component. While these operations add cost, the designer must balance this against the potential added benefit to the engine and vehicle. If these value added operations are used to reduce component weight, the following benefits result:

- reducing reciprocating inertial forces on the engine,
- reducing the amount of counterweight needed in the crank counterweight,
- reducing the vibration transmitted to the vehicle, improving NVH,
- reducing the amount of support structure needed in the vehicle.

Additional cost spent here has a leveraging affect on reducing weight and cost elsewhere in the vehicle.

16.7.5 Typical Bearing Journal Tolerances

There are a number of factors influencing the required bearing clearance, and the tolerance required to achieve this. The material of the cylinder block, connecting rod, and crankshaft will affect the overall system stiffness; and the geometry of each component will affect the component stiffness and individual contribution. The overall engine geometry, such as rod-to-stroke ratio or bore-to-stroke ratio, and engine combustion pressure will affect component loading. The maximum engine operating speed and weight of piston assembly and connecting rod assembly, will affect engine inertial loading. The surface finish of the bores will affect the fluid film bearings, as local high spots will decrease film thickness. The surface finish of the supporting bores will affect contact area with shell bearings, and will impact fretting at the mating surfaces. Oil viscosity and additive packages and oil pressure will affect film strength. The number of cylinders in the engine, bearing bore-to-bore alignment becomes more important the longer the crankshaft and more bearings are used. Finally, engine operating and storage temperatures will affect bearing clearances, especially if different materials are used for crankshaft, connecting rods, and cylinder block and differential thermal effects take place. It is best to consult the bearing manufacturer for installed bearing clearances. Some representative starting values are shown in **Table 16.5**.

Table 16.5: Starting values for a steel crankshaft, cast iron connecting rod, cast iron cylinder block

Feature	Starting Ranges for Component Tolerance
Diameter	0.013-0.025mm or $0.1*D_{shaft}$ = xx μ-m
Circularity	<0.013mm for journal or bearing bore in housing, cannot be measured at ID of shell bearing due to non uniform thickness
Surface Finish	0.2-0.4 μ-m Ra with 0.8mm cutoff or better for the crankpin and main bearing journals. 1.6-2.5 μ-m Ra for cylinder block parent metal bore or connecting rod bore where journal bearings will be used.
Alignment	<0.050mm maximum overall misalignment down the length of the crankshaft. <0.025mm maximum misalignment on adjacent bores.

16.8 Analysis and Test

The typical analysis path is to evaluate each component individually, and then once a level of maturity is reach, combine the individual components into a system model. The crankshaft analysis typically starts with analysis of a simply supported, single throw. Once that is complete, a full crankshaft model is analyzed. Often a course mesh model of the crankshaft is analyzed to determine system natural frequencies for torsional calculations. Then the crankshaft, connecting rod, and cylinder block are combined in a system analysis. This is typically more complex, as the fluid film must be modeled as gap elements. Some system stiffness is contributed by the crankshaft, and some by the cylinder block.

There are two opposing design philosophies for crankshaft-cylinder block design, one of cylinder block guided stiffness, and another of crankshaft guided stiffness. Each of the different methods has one component significantly stiffer than the other. Regardless of method chosen, the goal is to have sympathetic deflection in the same direction between the housing and the shaft, to prevent edge loading of the bearings.

16.8.1 Description of boundary conditions, constraints

Often for a first analysis, a simply supported crankshaft throw is evaluated at location of peak cylinder pressure, and peak inertial load cases. The mesh is refined in the critical fillet transitions to the journal bearings. A simply supported boundary condition at the midspan of the journal bearing will allow the crankshaft journal to tip in the bearing bore of the cylinder block as illustrated in **Figure 16.51**. This tipping will tend to over-predict the stress in the crankshaft fillets.

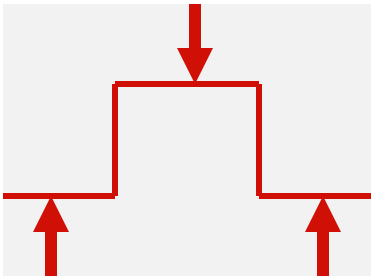

Figure 16.51: Simply supported boundary condition

The next level of refinement will add gap elements to simulate the fluid film bearings as indicated in **Figure 16.52**. This analysis takes into account the stiffness contribution of the cylinder block.

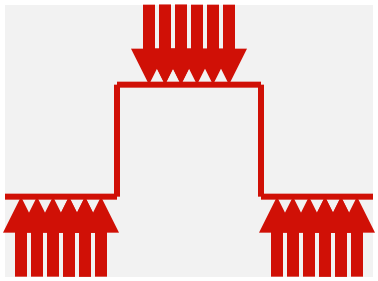

Figure 16.52: Analysis of crankshaft with fluid film bearings and housing.

If further refinement is required, the crankshaft and connecting rod loads are evaluated for a full 720° cycle for a four-stroke engine. This is important for fatigue calculations, as the loads fully reverse several times in the four stroke cycle.

16.8.2 Component Testing

If a crankshaft or connecting rod fails during engine testing, the results are usually catastrophic! If either component fails, many engine components are damaged beyond repair: crankshaft, cylinder block, connecting rod, cylinder head, valvetrain, etc. For this reason, crankshafts and connecting rods are typically subjected to component tests to prove their reliability, prior to exposing an expensive prototype engine to destruction.

Various servo-hydraulic rigs are used for component level testing. The crankshaft is usually evaluated for torsional strength and bending resistance at the crankpin. For torsional testing, it is usually supported at the main bearings, fixed at the power take off, and a firing pressure load applied at the crankpin for torsional testing. The bending load at the crankpin can either be simulated by fixing the crank near TDC and loading via a driven connecting rod, or can be subjected to moment by bending the crankshaft from one main bearing to another as represented in **Figure 16.53**. A single throw section is rigidly mounted in a heavy fixture that is then suspended as shown. By making the fixture mass large it will resonate at a very high natural frequency. Once this frequency is identified high fillet stress can be achieved with a very low driving force. Strain gauges

are added in the fillet region to drive the testing apparatus, or to assess the impact and sensitivity of different fillet radii under a given load. By varying the magnitude of loading at this frequency an 'S-N' diagram can be generated specific to the crankshaft section. The cycle accumulation rate is so high that the number of cycles the crankshaft would accumulate over its entire life in an engine can be accumulated in a matter of hours. The 'S-N' diagram results can be compared with the actual stresses seen by the crankshaft in the engine to determine the actual fatigue life. The rig test method described here is so easily done that it can be used for production quality checking as well. Production samples can be tested and overlaid on the 'S-N' diagram to quickly identify shifts that might occur due to casting or forging problems, material alloy changes, or grinding, hardening, shot peening, or cold rolling process control problems.

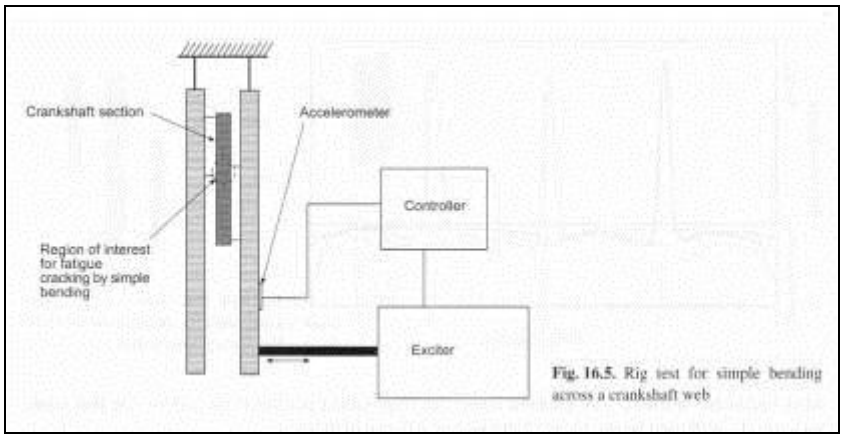

Figure 16.53: Rig test for…

Connecting rods are usually less sophisticated to test. A load is applied at the piston pin bushing, axial to the main beam of the rod. The crankpin end of the rod is fixed by a shaft of the same diameter of the crankpin to limit bore distortion. These tests are sometimes accelerated by inputting a force at the natural frequency of the component. An enhancement of this test is to mount the crankpin end of the rod off center from the piston pin end, and this can simulate axial as well as bending load due to rod whip as presented in **Figure 16.54**.

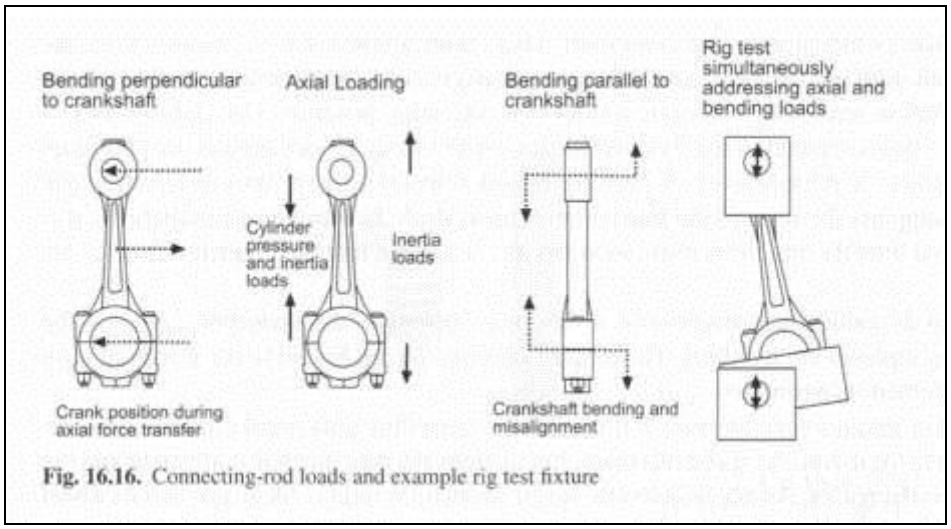

Figure 16.54: Connecting-rod loads…

Once individual component testing is passed, system level tests can begin. These can again be servo-hydraulic, where a hydraulic cylinder applies load to simulate combustion to a short block assembly of crankshaft, connecting rods, and cylinder block. Or, the short block can be rotated on a motoring rig, where the engine is spun by an electric motor without combustion taking place. This also allows the verification of the lubrication and breathing systems, and the measurement of engine friction. A disadvantage of a motoring rig test is the lack of combustion forces. This will under-represent the force due to combustion, but will amplify the loading due to inertia since gas forces will not counteract inertia during TDC power stroke.

These system level tests allow easier access to components for strain measurement. The use of strain gages and telemetry or slip rings are also methods to obtain information. Finally, a specialty device known as a "grasshopper linkage" can be used to take direct measurement of strain on a moving connecting rod. This is a two link assembly with one end attached to the connecting rod, and one end attached to a fixed point in the engine. This removes the need to have strain gauge wires rotate around the crankshaft, and once assembled and moving resembles the rear leg of a grasshopper.

Once these components have completed testing, they are cleared for use on the engine dyno. Typically, low speeds are evaluated first, and load and RPM are gradually increased as confidence grows.

16.9 Recommendations for Further Reading

A. SAE 2002-01-0770, 2002 Dubensky, R.G., "Crankshaft Concept Design Flowchart for Product Optimization,"
B. *Engine Connecting Rod for High Performance Applications and Method of Manufacture*, R. Weaver, US Patent 2008/0282838 A1

Connecting Rod Optimization for Weight and Cost Reduction, SAE 2005-01-0987, P. Shenoy, A. Fatemi

The following paper provides a design and development flowchart specifically addressing crankshafts. The level of detail provided will be especially appreciated by a first-time crankshaft designer.

> Dubensky, R.G., "Crankshaft Concept Design Flowchart for Product Optimization," SAE 2002-01-0770, 2002.

Although this is an older paper it provides a good summary of the dimensional details and design variables that determine crankshaft fatigue life.

> Shaw, T.M., Richter, I.B., "Crankshaft Design Using a Generalized Finite Element Model," SAE 790279, 1979.

The following three papers summarize crankshaft development for new automobile engines. The first is for a V6 engine and the second an in-line four. The third paper, again for a V-6 engine, emphasizes NVH considerations.

> Paek, Seong-Youn, "The Development of the New Type Crankshaft in the V6 Engine, SAE 990051, 1999.
>
> Fujimoto, T., Yamamoto, M., Okamura, K., Hida, Y., "Development of a Crankshaft Configuration Design," SAE 2001-01-1008.
>
> Druschitz, A.P., Warrick, R.J., Grimley, P.R., Towalski, C.R., Killion, D.L., Marlow, R., "Influence of Crankshaft Material and Design on the NVH Characteristics of a Modern, Aluminum Block, V-6 Engine," SAE 1999-01-1225, 1999.

The following papers discuss crankshaft durability. The first discusses resonant bending fatigue testing, and the second discusses crankshaft forging and grain flow.

> Yu, V., Chien, W.Y., Choi, K.S., Pan, J., Close, D., "Testing and Modeling of Frequency Drops in Resonant Bending Fatigue Tests of Notched Crankshaft Sections," SAE 2004-01-1501, 2004.
>
> Shamasundar, S., "Prediction of Defects and Analysis of Grain Flow in Crankshaft Forging by Process Modeling," SAE 2004-01-1499, 2004.

Shot peening is an important process for applying compressive residual stress to crankshaft fillets, thus improving their fatigue life. This paper presents a detailed look at the process, the resulting surface characteristics, and the effect on fatigue life.

> Wandell, James L., "Shot Peening of Engine Components," ASME Paper No. 97-ICE-45, 1997.

This presentation, available through the Gas Machinery Institute provides an extremely detailed look at Torsional vibration in engines, and the effects of various vibration dampers.

Feese, Troy, and Hill, Charles, "Guidelines for Preventing Torsional Vibration Problems in Reciprocating Machinery," presented at Gas Machinery Conference, Nashville, Tennessee, 2002.

The following paper presents a recent study of connecting rod fatigue in powdered metal and forged designs. The next paper discusses fracture-split connecting rod design. The text then listed devotes a chapter to connecting rod fatigue, and rig testing for rod development.

Afzal, A., Fatemi, A., "A Comparative Study of Fatigue Behavior and Life Predictions of Forged Steel and PM Connecting Rods," SAE 2004-01-1529, 2004.

Park, H., Ko, Y.S., Jung, S.C., Song, B.T., Jun, Y.H., Lee, B.C., Lim, J.D., "Development of Fracture Split Steel Connecting Rods," SAE 2003-01-1309, 2003.

Wright, Donald H., *Testing Automotive Materials and Components*, SAE Press, Warrendale, Pennsylvania, 1995.

"When Splines Need Stress Control" by Darle W. Dudley, Product Engineering, 12/23/57.

McCardell, W., Mahoney, J., and Cameron, D., "Design Practice Automotive Driveline Splines and Serrations," SAE Technical Paper 680009, 1968, doi:10.4271/680009.

A Comaprion of manufacturing Techniques in the Connecting Rod Industry, Colorado School of Mines, D. Visser, 2008